5

Structural Features of Starch Granules I

Serge Pérez[1], *Paul M. Baldwin*[2] *and Daniel J. Gallant*[3]

[1]*Centre de Recherches sur les Macromolécules Végétales (affiliated with the Université Joseph Fourier, Grenoble), CNRS, Grenoble, France*
[2]*Centre de Recherches Agro-Alimentaires, INRA, Nantes, France*
[3]*Centre de Recherches Agro-Alimentaires, INRA, Nantes, France*

I. Introduction

As this chapter and Chapter 6 are read it should be remembered that, as far as is known, the amylose and amylopectin molecules, the granule structure, and the natures and amounts of the lipid and protein molecules present in granules vary with the botanical source of the starch, i.e. are unique to each type of starch. Therefore, what has been

Starch: Chemistry and Technology, Third Edition
ISBN: 978-0-12-746275-2

discovered about the structural features of one type of starch does not necessarily apply to other types of starch. At this time the generalities that can be attributed to all starch granules, i.e. features that apply to all granules of all starches, are unknown.

The starch granule is nature's chief way of storing energy over long periods in green plants. The granule is well-suited to this role, being insoluble in water and densely packed, but still accessible to the plant's catabolic enzymes. Starch granules are mainly found in seeds, roots and tubers, but are also found in stems, leaves, fruits and even pollen. Starch granules occur in all shapes and sizes (spheres, ellipsoids, polygons, platelets, irregular tubules); their long dimensions range from 0.1 to at least 200 μm, depending on the botanical source.[1] Differences in external granule morphology are generally sufficient to provide unambiguous characterization of the botanical source, via optical microscopy.

Native starch granules have a crystallinity varying from 15% to 45%,[2] thus, most native starch granules exhibit a Maltese cross when observed under polarized light (Figure 5.1). Theoretically, the positive birefringence indicates a radial orientation of the principle axis of the crystallites. However, birefringence remains unchanged on both polar and equatorial sections of elongated starch granules,[1] indicating that crystallites are extremely small and exhibit multiple orientations, which interfere during observations. From the level of starch crystallinity, it is clear that most starch polymers in the granule (on average ~70%) are in an amorphous state.[3] Native granules do, nevertheless, yield x-ray diffraction patterns, which although they are generally of

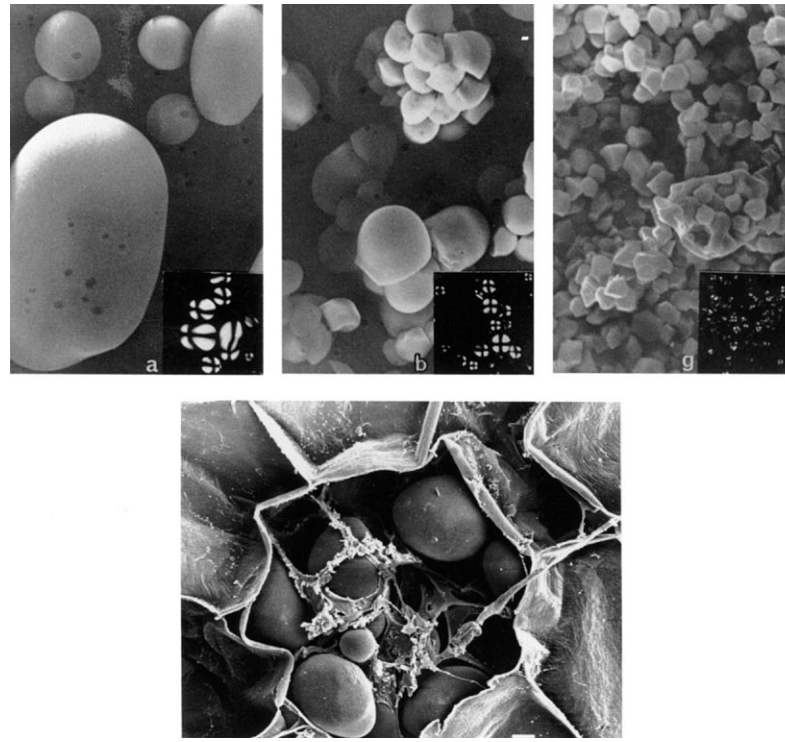

Figure 5.1 Raw starch granules observed by scanning electron microscopy: (a) potato; (b) cassava; and (g) rice starches. The corresponding granules under polarized light are shown in insets. Lowest figure shows SEM of *in situ* granules in potato parenchyma cell. (Reproduced with permission from reference 1)

low quality, can be used to identify the several allomorphs.[4] Classification based on diffractometric spectra does not follow the morphological classification, but is able to group most starches conveniently according to their physical properties. Generally, most cereal starches give the so-called A-type pattern; some tuber starches (e.g. potato) and cereal starches rich in amylose yield the B-type pattern, while legume starches generally give a C-type pattern.

The two major macromolecular components of starch are amylose and amylopectin (Figure 5.2). They can be identified only after separation following solubilization

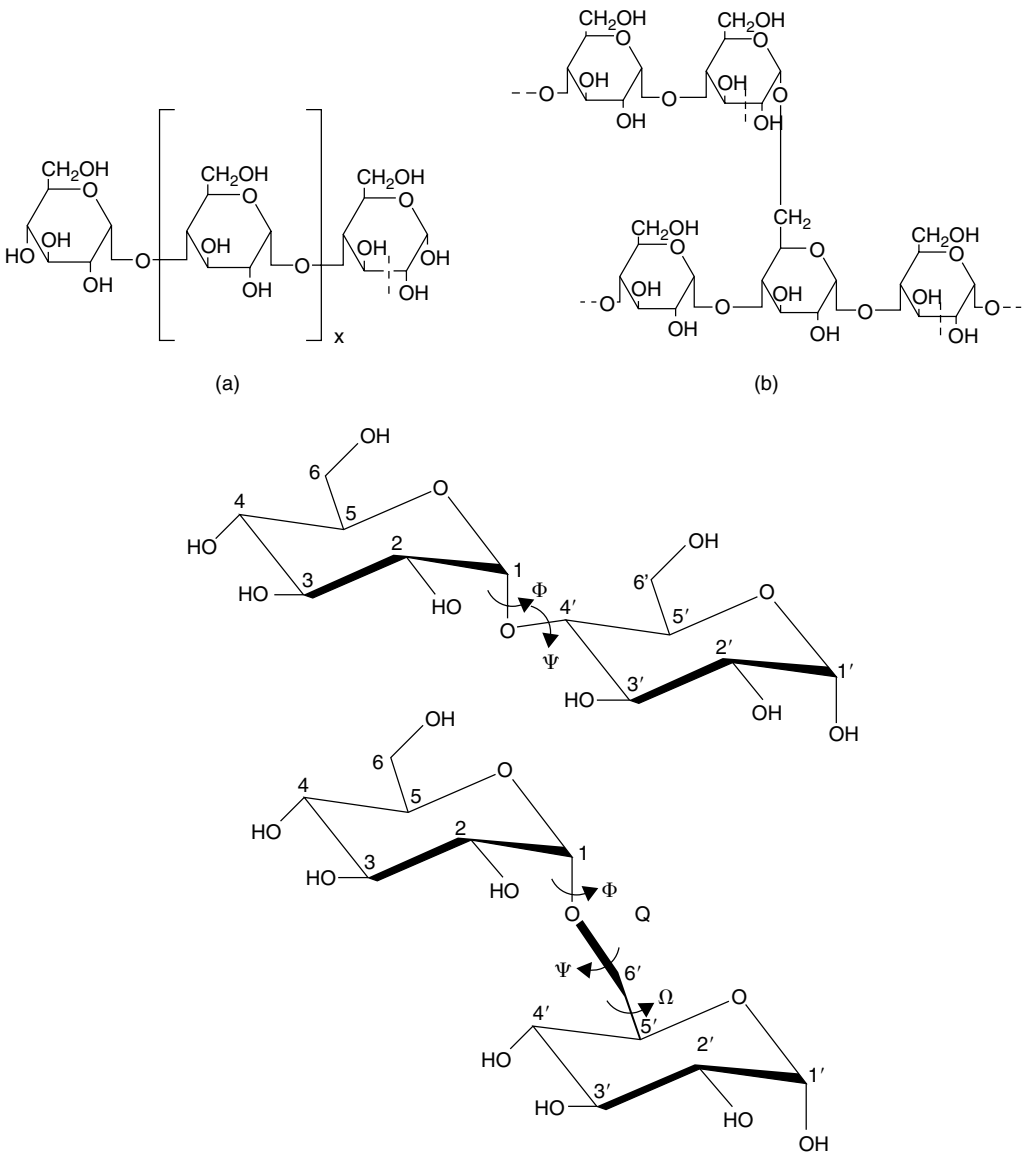

Figure 5.2 Schematic diagram of (a) amylose; and (b) amylopectin with a branch point at the O6 position. (c) Schematic representation of the disaccharide components of starch: maltose [αGlc-(1→4)Glc] and isomaltose [αGlc(1→6)Glc] along with the torsion angles that define the conformations at the glycosidic linkage between two contiguous residues: Φ = O-5-C-1-O-1-C-4′, Ψ = C-1-O-1-C-4′-C-5′, Ω = O-1-C-6′-C-5′-O-5′.

of the granule. Amylose is the predominantly linear (1→4)-linked α-glucan and can have a degree of polymerization (DP) as high as 600. Amylopectin, α(1→4)-linked α-glucan with α-(1→6) branch points, is the major component of the granule (30– > 99%). With a molecular weight ranging from $50 - 500 \times 10^6$, it is one of the largest natural polymers known. Amylopectin contains about 5% of branch points, which, as compared to amylose, impart profound differences in physical and biological properties. Following sequential analysis of the macromolecule, it becomes apparent that the molecule possesses several populations of polymer chains which can be classified as short chains ($12 < DP < 20$), long chains ($30 < DP < 45$), and very long chains having an average $DP > 60$. The chains are further classified into A-, B- and C-chains, where A-chains do not carry any other chains, B-chains carry one or more chains, and the C-chain is the original chain carrying the sole reducing end (Figure 5.3). The current and widely accepted model is the cluster model.[5–11] In this model, the branch points in the amylopectin molecules are not randomly distributed, but are 'clustered.' Clusters of many short linear chains (with DP between 12 and 70)[12–14] are thought to be more crystalline than the branching regions, and to form thin crystalline lamellae (5–7 nm thick) which alternate with less crystalline (3–4 nm thick) regions composed of the branch points. These two domains appear to exist in two main directions, with a relative angle between them of about 25°.[3] Hizukuri[15] demonstrated that B-chains of amylopectin can participate in more than one crystalline side chain cluster. They, therefore, proposed a revised model of amylopectin structure and classified the B-chains according to the number of side chain clusters in which they participate. B1-chains participate in one cluster; B2- and B3-chains extend into two and three clusters respectively, and B4-chains link four or more clusters.

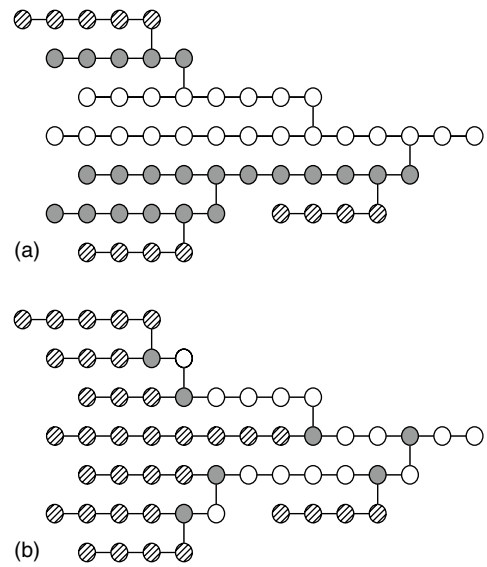

Figure 5.3 Schematic representation and definition of the different chains constituting the amylopectin macromolecule: (a) gray circles represent *A*-chains, dotted circles *Ba*-chains, and white circles *Bb*-chains; (b) gray circles represent external chains, black circles branch points, and white circles internal chains.

It has been estimated by Manners[16] that 80–90% of the total number of chains in an amylopectin molecule are part of side chain clusters, while the remaining 10–20% of chains form inter-cluster connections. Thus, substantial progress in understanding the basic structure of amylopectin has been made. Although the three-dimensional structure of amylopectin in the granule is not yet known, there is evidence that it is a two-dimensional ellipsoid.[17–19]

II. Granule Architecture

1. An Overview of Granule Structure

At the lowest level of structure, most starch granules are made up of alternating amorphous and crystalline shells which are between 100 and 400 nm thick.[11,12,20] These structures are termed 'growth rings.' Radial organization of amylopectin molecules within such structures is thought to cause optical polarization, since the visible optical polarization is in the order of the wavelength of visible light (100 to 1000 nm).[21] At a higher level of molecular order, x-ray diffraction investigations[22–24] in association with electron microscopy[20,25] indicate a periodicity of 9–10 nm within the granule. The periodicity is interpreted as being due to the crystalline and amorphous lamellae formed by clusters of side chains branching off from the radially arranged amylopectin molecules, and appears to be a universal feature of starch granules, independent of botanical source. Furthermore, it suggests a common mechanism for starch deposition.[26]

2. Molecular Organization of Crystalline Structures

Good quality powder diffraction patterns can be obtained from starch granules subjected to mild acid-catalyzed hydrolysis to remove amorphous portions. Good powder diffraction patterns have also been obtained from crystallized short amylose chains (DP <50), either in the form of spherulites[27] or lamella single crystals.[28] These powder diffraction patterns are difficult to interpret, because of the complexity of the polymer structures. Fiber diffraction may complement the paucity of the data from powder diffraction. One fiber diffraction study was performed using the radial axis of a giant granule,[29] but in most cases the samples originate from a film cast from solutions of high DP amylose. Stretching the films aligns the crystallites' axes. The filaments give the same characteristic A- and B-diffraction patterns[30,31] as the short branch segments of amylopectin in granules. Similar observations can be made for single crystals grown *in vitro*[28] from monodisperse fractions of amylose having DP 15 and DP 30, which give rise to powder diffraction patterns typical of the A-type and B-type patterns, respectively (Figure 5.4).

The structure of A-type starch crystals was derived through the joint use of electron diffraction of single crystals, x-ray powder patterns decomposed into individual peaks, x-ray fiber diffraction data and extensive molecular modeling[32] (Figure 5.5). The density calculated for the crystalline region ($d = 1.48$) is reasonably close to the observed density, and indicates that there are 12 glucosyl units and 4 water molecules in the unit cell. Intra- and inter-molecular energy calculations showed that

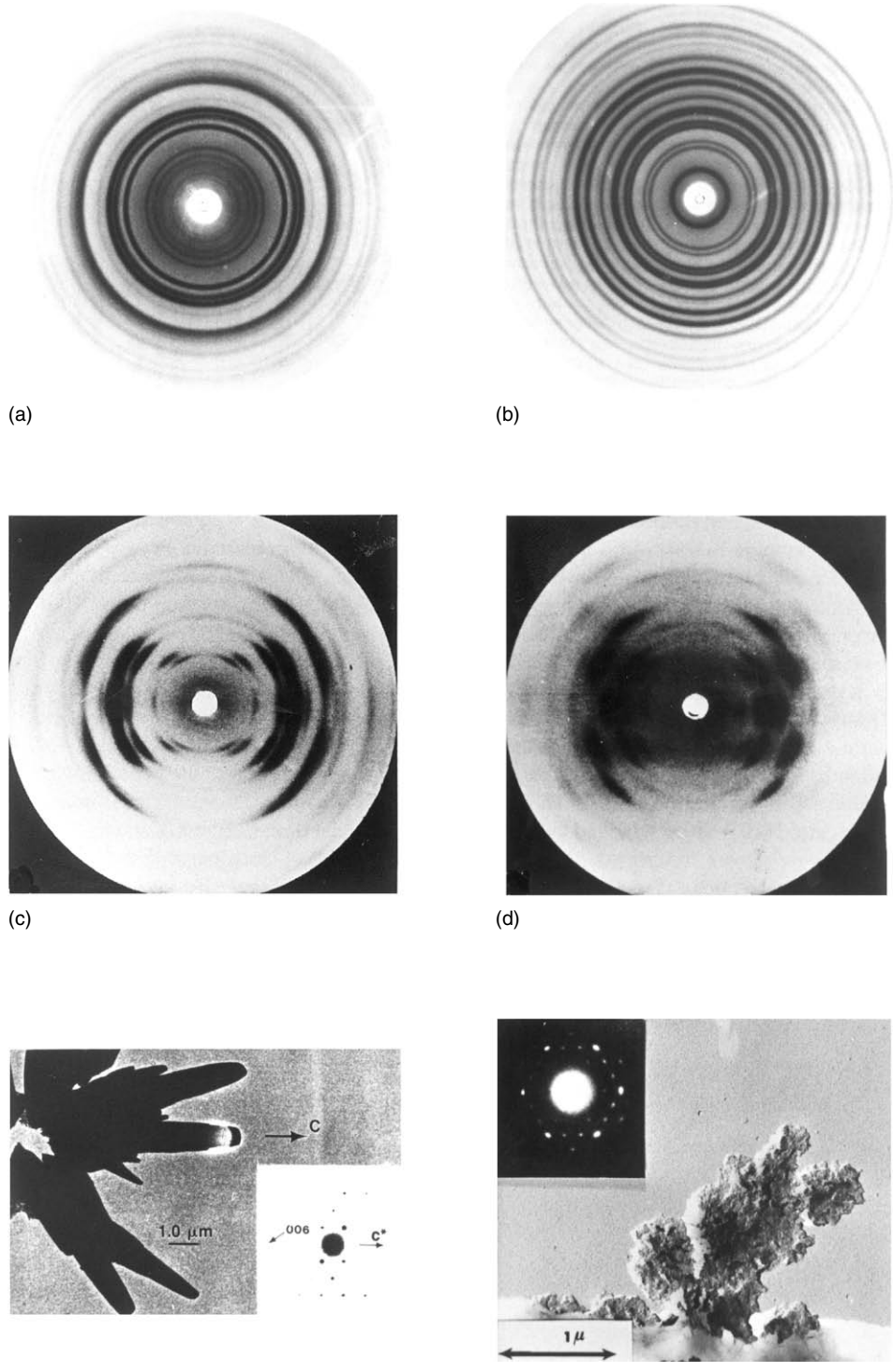

Figure 5.4 X-ray powder diffractogram recorded for: (a) A-type amylodextrins; and (b) B-type amylodextrins grown as spherulites. X-ray fiber diffraction patterns (fiber axis vertical) for: (c) A-amylose (fiber spacing 1.04 nm); and (d) B-amylose (fiber spacing 1.05 nm). (Reproduced with permission from references 30 and 31). Microcrystal of: (e) A-starch; and (f) B-starch observed by low dose electron microscopy. Inset: the electron diffraction diagrams recorded under frozen wet conditions (e). (Reproduced with permission from references 32 and 34)

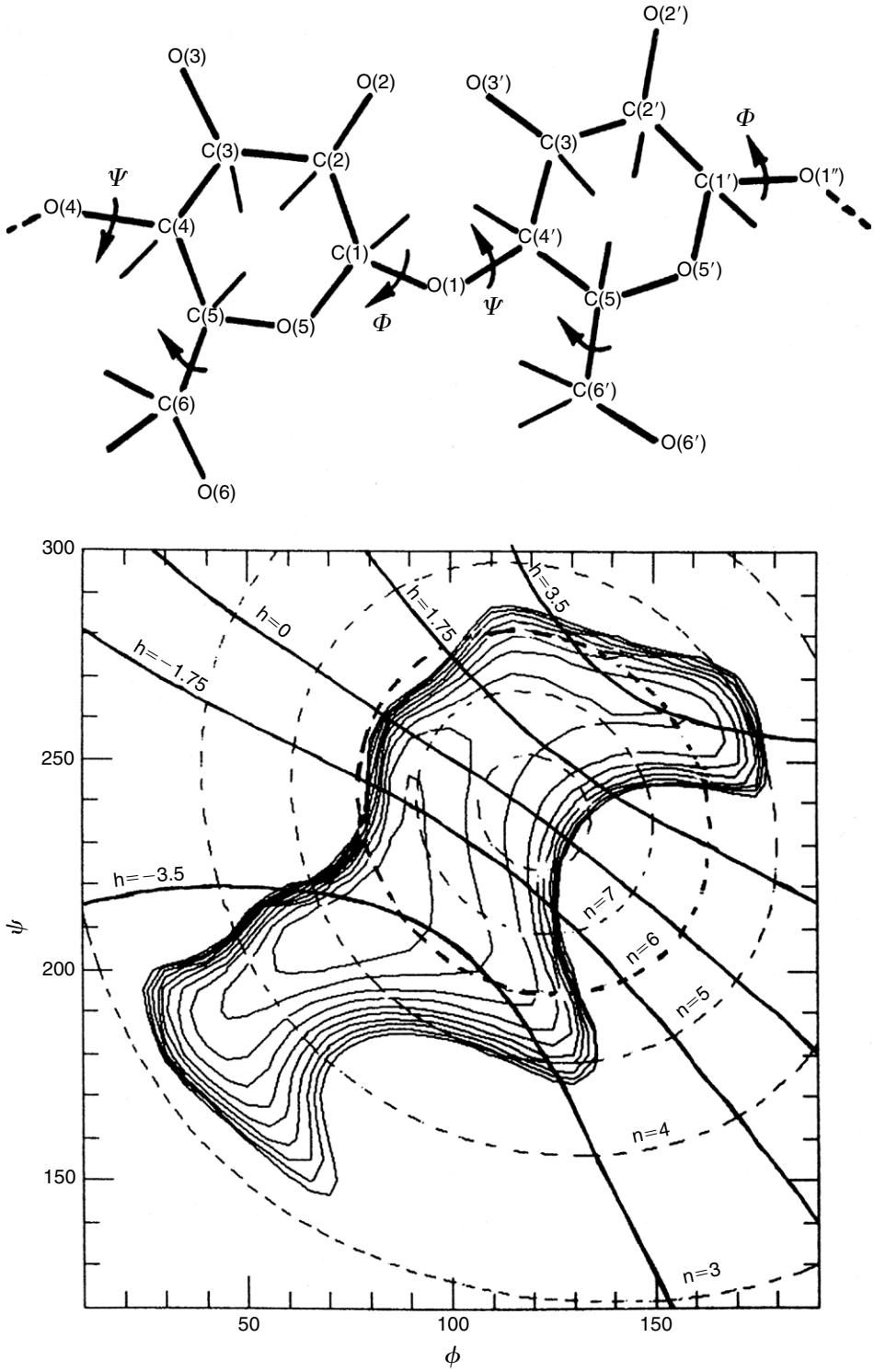

Figure 5.5 Selected iso-*n* and iso-*h* contours superimposed on the potential energy surface for maltose computed as a function of Φ and Ψ glycosidic torsion angles. Iso-energy contours are drawn by interpolation of 1 kcal/mol with respect to the energy minimum (*). The iso-$h = 0$ contour divides the map into two regions corresponding to right-handed ($h > 0$) and left-handed ($h < 0$) chirality.

the only suitable models for the chain structure were left-handed, parallel-stranded, double helices. Each strand repeats in 2.138 nm, but is related to the other strand by a two-fold axis of rotation, yielding the apparent fiber repeat distance of 1.069 nm. There are no intra-chain hydrogen bonds, but there is an O-2 … O-6 hydrogen bond between the two strands. The double helix is very compact, and there is no space for water or any other molecule in the center (Figure 5.6a).

The monoclinic space group B_2 ($a = 2.124$ nm, $b = 1.172$ nm, $c = 1.069$ nm, $\gamma = 123.5°$) requires that the asymmetric unit contains a maltotriosyl unit, and that the packing contains one double helix at the corner and another at the center of the unit cell. Synchrotron radiation microdiffraction data has confirmed these crystallographic assignments.[33] The space group also demands that all helices be parallel (Figure 5.6b). There are hydrogen bonds between these helices, either direct or through the four water molecules in the unit cell. These water molecules are buried deep in the crystal structure, and it is impossible to remove them without complete destruction of the crystalline structure (Figure 5.6).

The structure of B-type starch crystals was established by combining the set of experimental data derived from x-ray fiber and electron diffraction crystallography via an appropriate molecular modeling technique.[34] The chains in B-type starch are also organized in double helices, but the structure differs from A-type starch in crystal packing and water content, the latter ranging from 10% to 50%. The crystalline unit cell is hexagonal ($a = b = 1.85$ nm, $c = 1.04$ nm), space group $P6_1$. Double helices are connected through a network of hydrogen bonds that form a channel inside the hexagonal arrangement of six double helices (Figure 5.6c). This channel is filled with water molecules, half of which are bound to amylose by hydrogen bonds and the other half to other water molecules. Thus, with a hydration of 27%, 36 water molecules are located in the unit cell between the six double helices, creating a column of water surrounded by the hexagonal network. There is no indication of disorder of these water molecules, agreeing with an NMR investigation that indicates that 'freezable water' can be observed only when the hydration is above 33%.[35]

The structural features of A-type and B-type starch crystallites can be compared at the molecular level. The double helices in both A- and B-type starches are left-handed, almost perfectly six-fold structures, with a crystallographic repeat distance of about 1.05 nm. The geometry of the single strands is similar to the geometry of KOH amylose and amylose triacetate. However, in the KOH and triacetylated structures, the amylose chain exists as a single strand. In the A and B allomorphs, the observed space group imposes parallel arrangement of all double helices. Double helices of both forms are packed in hexagonal or pseudohexagonal arrays. The void in the lattice of B-type starches, which accommodates numerous water molecules, is not present in A-type starches. In both arrangements there is a pairing of double helices that corresponds to 1.1 times the distance between the axes of the two double helices. A relative translational shift of 0.5 nm along the orientation of the chains allows very close nesting of the crests and troughs of the paired double helices. Such a dense association, which is strengthened by O-2 … O-6 and O-4 … O-3 hydrogen bonding, corresponds to the most energetically favored interactions between two double helices, as shown by theoretical calculations.[36]

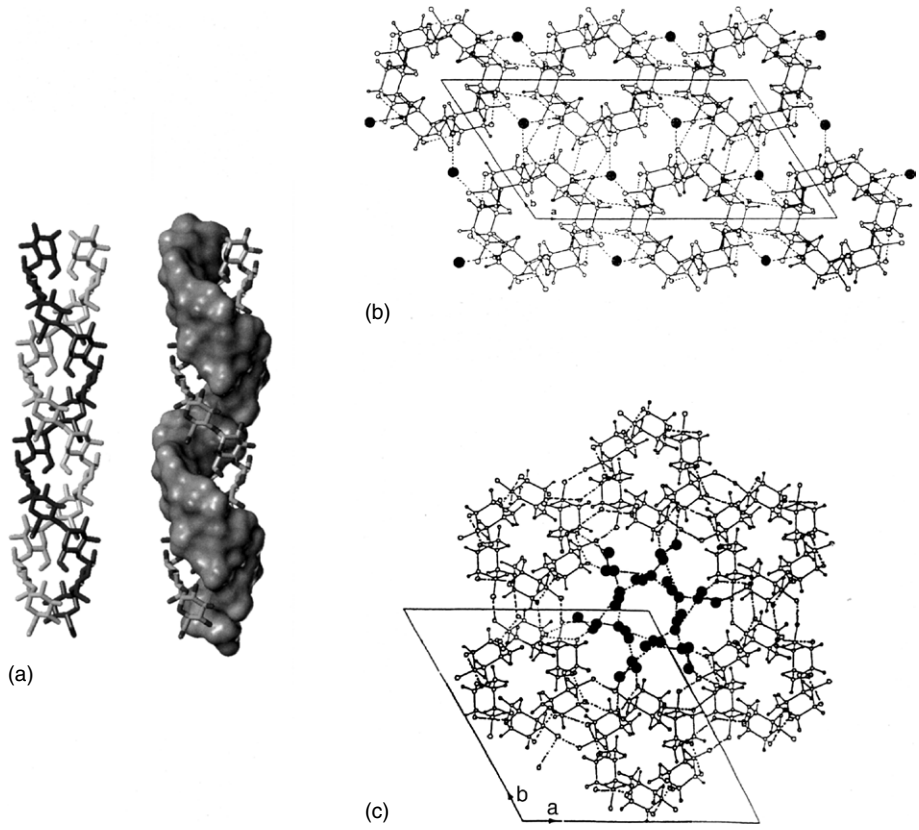

Figure 5.6 (a) Molecular drawing for the double helix found in A and B starches. Each single strand of an amylosic chain is in the left-handed conformation having six-fold symmetry, repeating in 2.1 nm; the double helix is generated by association of two single strands through two-fold symmetry. (b) Structure of A starch. Chains are crystallized in a monoclinic lattice. In such a unit cell, 12 glucopyranosyl units are located in two left-handed, parallel-stranded double helices, packed in a parallel fashion. For each unit cell, four water molecules (closed circles) are located between the helices. Projection of the structure onto the (a, b) plane. Hydrogen bonds are indicated as broken lines. (Reproduced with permission from reference 32) (c) Structure of B starch. Chains are crystallized in a hexagonal lattice, where they pack as an array of left-handed parallel-stranded double helices in a parallel fashion. 36 water molecules represent 27% hydration. Half the water molecules are tightly bound to double helices; the remainder form a complex network centered around the six-fold screw axis of the unit cell. Projection of the structure onto the (a, b) plane. Hydrogen bonds are indicated as broken lines. (Reproduced with permission from reference 33)

Conditions required to generate A- and B-type crystal conformations are reasonably well-understood. Under cool, wet conditions (such as in a potato tuber), B-type starch crystals form, while in warmer, drier conditions (e.g. in a cereal grain), the A allomorph is preferred. Chain length also affects the selection of crystal form, chains of DP <10 do not crystallize, chains with a DP from 10 to 12 tend to form A-type crystals, and chains with a DP >12 tend to yield the B form.[37,38] This is likely the result of differences in loss of entropy on crystallization experienced by chains of different lengths.[39] An irreversible transition from B-type starch to A-type starch can be accomplished under conditions of low humidity and high temperature. This so-called

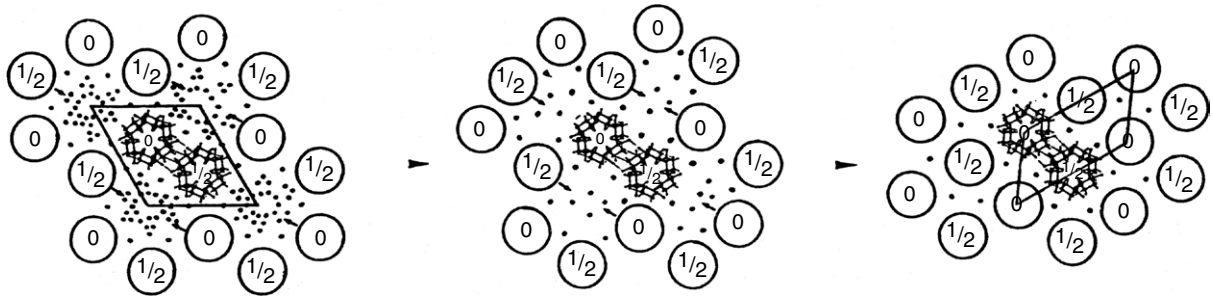

Figure 5.7 Model of the polymorphic transition from B-type to A-type starch in the solid state. The parallel double helices which form the duplex are labeled 0 and ½, indicating their relative translation along the c axis. Water molecules are shown as dots. (Reproduced with permission from reference 159)

heat–moisture treatment involves rearrangement of the pairs of double helices[14,40] (Figure 5.7).

Crystal form is also considered to be an important contributing factor in determining overall granule properties. Thus, in starches which display the A-type crystal form, the gelatinization temperature generally tends to increase with increasing overall crystallinity of the granule, while the reverse is generally true for starches displaying the B-type crystal form.

3. Crystalline Ultrastructural Features of Starch

Most common starch granules are much too small to be studied individually by diffraction analysis or solid-state polymer techniques such as spectroscopy. Until recently, there was only a single case where an oriented x-ray diagram had been obtained from an isolated starch granule. This diffraction diagram was obtained in 1951[29] with an x-ray micro-camera from a gigantic granule extracted from the pseudobulb of the orchid *Phajus grandifolius*. The results showed that the molecular orientation of the diffracting material was perpendicular to the growth rings of this unusually large granule. Characterization of starch granules that are elliptical in shape with their long axis never greater than 100 μm has now become possible through use of microfocus x-ray diffraction from synchrotron radiation. An x-ray beam of 2 μm full width, having flux of about 10^{10} photons/second/μm^2 (available at the European Synchrotron Radiation Facility in Grenoble, France), has been used to map the occurrence of crystalline regions within a single granule without subjecting the granule to any sample preparation. Oriented two-dimensional diffraction patterns can be obtained, yielding key information about the nature of the crystalline structure, along with its location and orientation with respect to the granule. Diffraction patterns can be collected at 10-μm steps across a single granule, thereby providing a complete mapping of the crystalline components (schematically represented in Figure 5.8). Individual wheat and potato starch granules have been subjected to such an investigation.[41,42] Individual diffraction patterns having unit cell dimensions in very good agreement with those of A- and B-type crystal structures[32,34] have been recorded on individual granules. The results establish, without any ambiguity, the

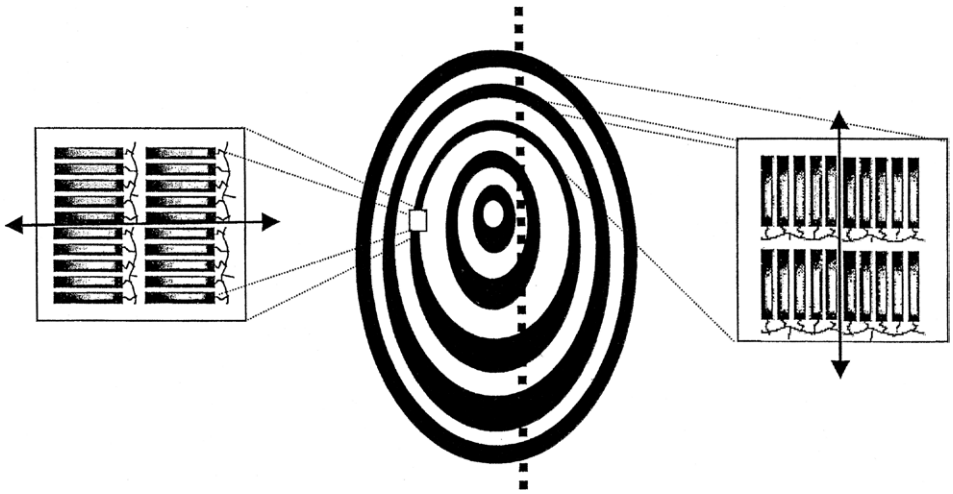

Figure 5.8 Granule in cross-section showing the orientation of amylopectin double helices in the crystalline lamellae. The dashed line indicates the path followed to obtain the diffraction diagram using a microfocus x-ray diffraction beam having a diameter of 2 μm. (Adapted with permission from reference 42)

orientation of amylopectin double helices in the crystalline lamellae (Figure 5.8). The most accurate mapping has been recorded for potato starch. Interestingly, these double helices do not point toward a single focus, but instead toward the surface of an inner ellipsoid. The helices are radially oriented, i.e. they are found to be perpendicular to the surface of the granule. This is in agreement with information derived from birefringence studies. At 10 μm resolution, there was no discontinuity of orientation (disclination or granule boundaries). This indicates a gradual change in the direction of the helices between 10 μm steps, consistent throughout with radial orientation.[42]

Microfocus synchrotron wide-angle diffraction mapping was also used to decipher the crystalline microstructure of granules from smooth pea, exhibiting so-called C-type polymorphism.[43] The specimen contained 60% A-type structure and 40% B-type structure, and these two crystalline phases co-existed within the same granule (Figure 5.9). The A allomorph was essentially located in the outer part of the granules, whereas the B-type was found mostly near their center. The diffraction diagrams for the A component were always poorly-oriented fiber patterns with the fiber axis systematically oriented toward the center of the granule. For the B allomorph in the center of the granule (where B-type cystallites are located), only powder diagrams could be observed. In in-between areas, the B component was much better oriented than the A component. These observations confirm the results of Bogracheva et al.,[44] who followed the loss of birefringence of granules during gelatinization in aqueous KCl solution, and found that the central part of smooth pea starch granules contained the B allomorph and the outer part the A allomorph. Together, these results provide a definite answer to the nature of the so-called C allomorph, i.e. that it is a combination of A- and B-crystalline constituents. This corroborates previous conclusions derived from molecular modeling which showed that the A and B arrangements were the only two possible crystalline arrangements of low energy.[36]

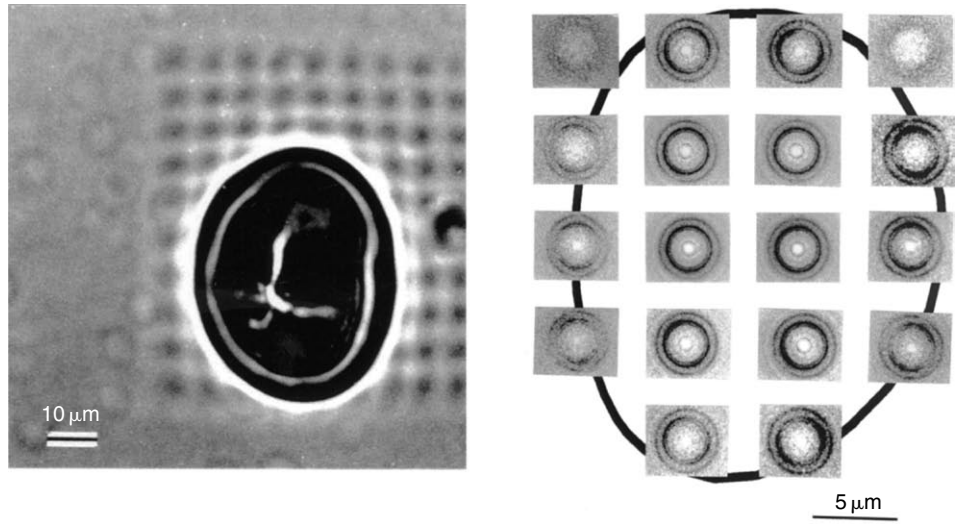

Figure 5.9 Distribution of the crystalline domains in pea starch: (a) optical micrograph of a typical sample of smooth pea starch after a 7 μm step irradiation with an x-ray beam of 2 μm diameter, each step consisting of a 16s exposure; (b) set of microfocus x-ray diffraction patterns recorded on a smooth pea starch granule. Each diagram corresponds to a diffraction area of ~3 μm^2; steps of 7 μm separate the diagrams. (Reproduced with permission from reference 41)

At the present time, the synchrotron microbeam has a diameter of around 2 μm. Such a size is small enough to assess gross ultrastructural features of the diffracting materials of individual starch granules. However, this beam size is still too large to assess the details of the crystalline micro-morphology of individual concentric layers (~500 nm in thickness) that are located within the granule. During scanning of a granule, several of these layers are diffracting at the same time. In the case of starch from smooth pea, it is impossible to assess whether the A- and B-phases are present within the same single layer of the granule or along a single cluster of amylopectin.

4. The Supramolecular Organization of Starch Granules

Even though some detailed information regarding starch polymer structures has been simulated at the atomic level by computer modeling, the structure of granules at the level of crystalline and amorphous domains (both on the lamella scale and that of the 'growth' rings) is less well-understood. Such knowledge is important for an understanding of the physical properties of starch. As stated above, small angle x-ray diffraction and electron microscopy have revealed a periodicity in the granule of about 10 nm, which has been explained by stacks of alternating thin crystalline and amorphous lamellae, as proposed in the cluster model of amylopectin.[9,16]

The structural characteristics of the branching areas of amylopectin are difficult to assess, since they are thought to be located in the amorphous regions between crystallites and since they constitute only a small fraction of the total molecule. Some basic structural features have, however, been established through computer modeling.[45] In particular it was found that, among the low-energy arrangements, one had

the side chains folded back onto the carrying chain, thereby producing dense, three-dimensional structures in which a parallel arrangement is achieved. Furthermore, the branching between the two strands of double helices was investigated. It was found that one particular set of conformations about the glycosidic linkages in the two strands could result in an arrangement such that double helical strands could be connected through an $\alpha-(1\rightarrow6)$ linkage with a minimum of distortion (Figure 5.10). This indicates that the branch points do not induce extensive defects in the double helical structure, but instead may serve to initiate the crystalline arrangement.

The concept of amylopectin forming double helices easily integrates into the currently-accepted cluster model, with the short linear chains of the branches being intertwined into double helices, while the branch points are located in the more amorphous regions between the clusters of double helices. Understanding that parts of amylopectin molecules are capable of forming double helices explains the apparent anomaly that a branched polymer is the source of structural order within granules.

According to Hizukuri,[15] amylopectin molecules of A-type starches have shorter constitutive chains and a larger short-chain fraction than amylopectin molecules of the B-type starches. Jane et al.[46] determined that A-type starches had branch points scattered in both amorphous and crystalline regions, while B-type starch had the most branch points clustering in amorphous areas. It was concluded that the branching pattern of amylopectin played a key role in determination of the type of crystallinity.[44] This point of view was confirmed through an investigation of the relationship of the distance between branching points in a cluster to the crystal pattern.[47] The study was performed on two allomorphs, maize double mutants of A- and B-types (*wxdu* and *aewx*, respectively). It was shown that the branching zone of clusters in A-type clusters was larger, but with a shorter distance between branching points, than in the B-type branching zone of clusters. These results indicate that both chain length and $(1\rightarrow6)$ linkage distribution are determinants of cluster features.

A further interesting observation regarding starch granule molecular order was gained by solid-state ^{13}C-NMR investigations,[48] which allow an assessment of the ratio of single to double chains in a given starch sample. The investigation suggested that the level of helical order is often significantly greater than the extent of crystalline order, which means that starch granules contain many double helices that are not part of extended crystalline arrays. This observation is assumed to be relevant to the amylopectin component of the granule (since amylose is not thought to be in the double helical state), and suggests that much of the amylopectin in the more semicrystalline shells of the granule is in a double helical form. As mentioned above, computer modeling[45] supports such a view, i.e. that double helices in amylopectin are sustainable in terms of molecular energetics, even at branch points that are located in the amorphous regions of lamellae (Figure 5.11).

Recent advances in molecular modeling offer new possibilities to investigate further the nature and importance of both branch points and amorphous/crystalline interfaces in starch granules. In approaching these questions, it is wise to adopt the attitude that one is not searching for single answers, but for all indications that would lead to a clearer image of how starch macromolecules are arranged and interact in nature. To this end, subunits of single helices, double helices and branch points were

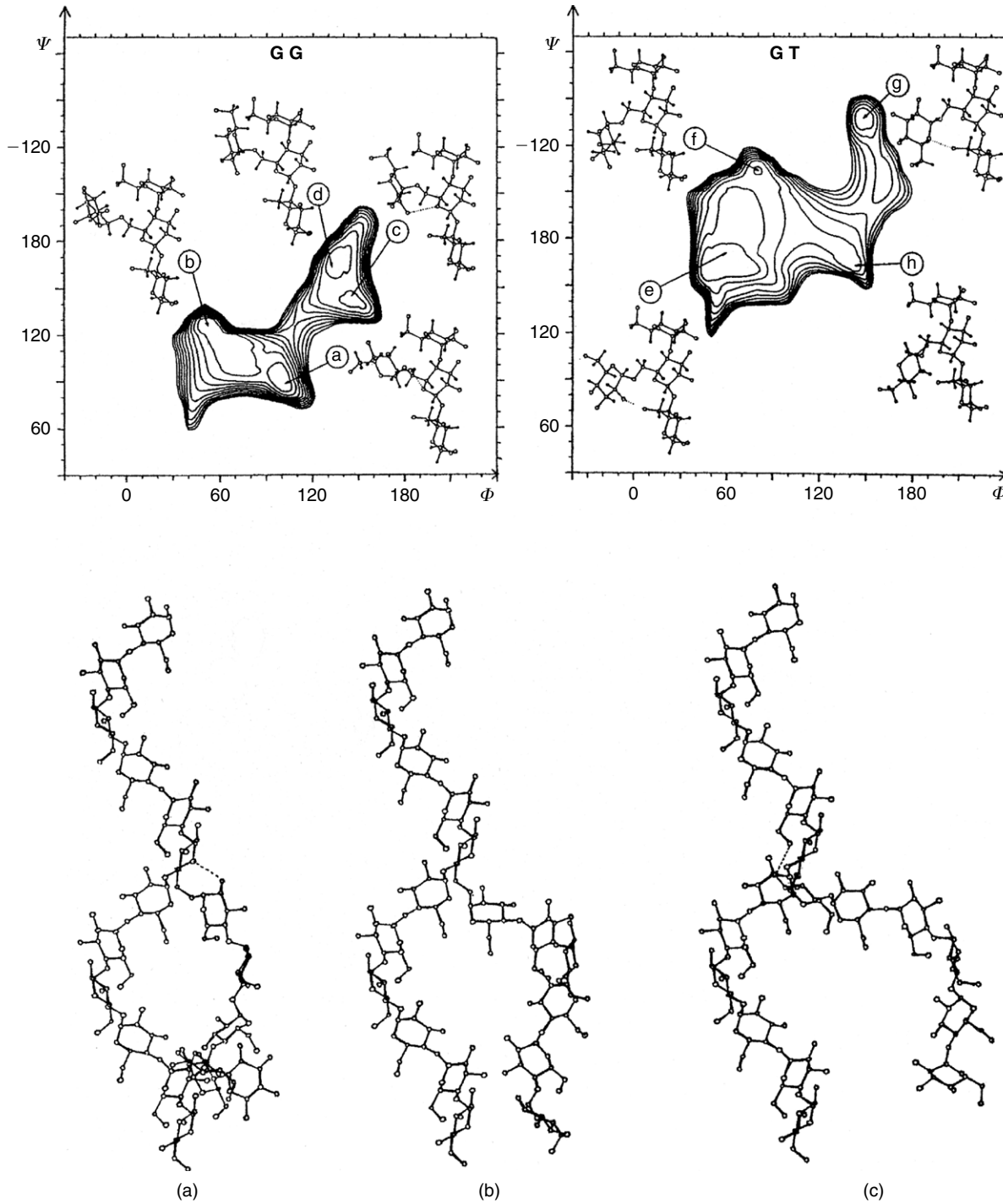

Figure 5.10 Branching points of amylopectin. (a) Two-dimensional, iso-energy surfaces for the (1→6) linkage of a 6^2-α-D-glucosylmaltotriose molecule. The maltotriose moiety was kept in the conformation observed for crystalline starch. Two orientations for the Ω angles were taken into account (GG; *gauche-gauche* orientation: $\Omega = -60°$) and (GT, *gauche-trans* orientation: $\Omega = 60$). Iso-energy contours were drawn by extrapolation of 1 kcal/mol with respect to the absolute minimum of each map. Four molecules, corresponding to conformations of lowest energy are shown on each map. (b) Three models of singly-branched amylopectin obtained by propagating amylosic chains from three low-energy conformations of the tetrasaccharide model of the branch point. The main chains have 12 glucosyl units and the side chain 6.

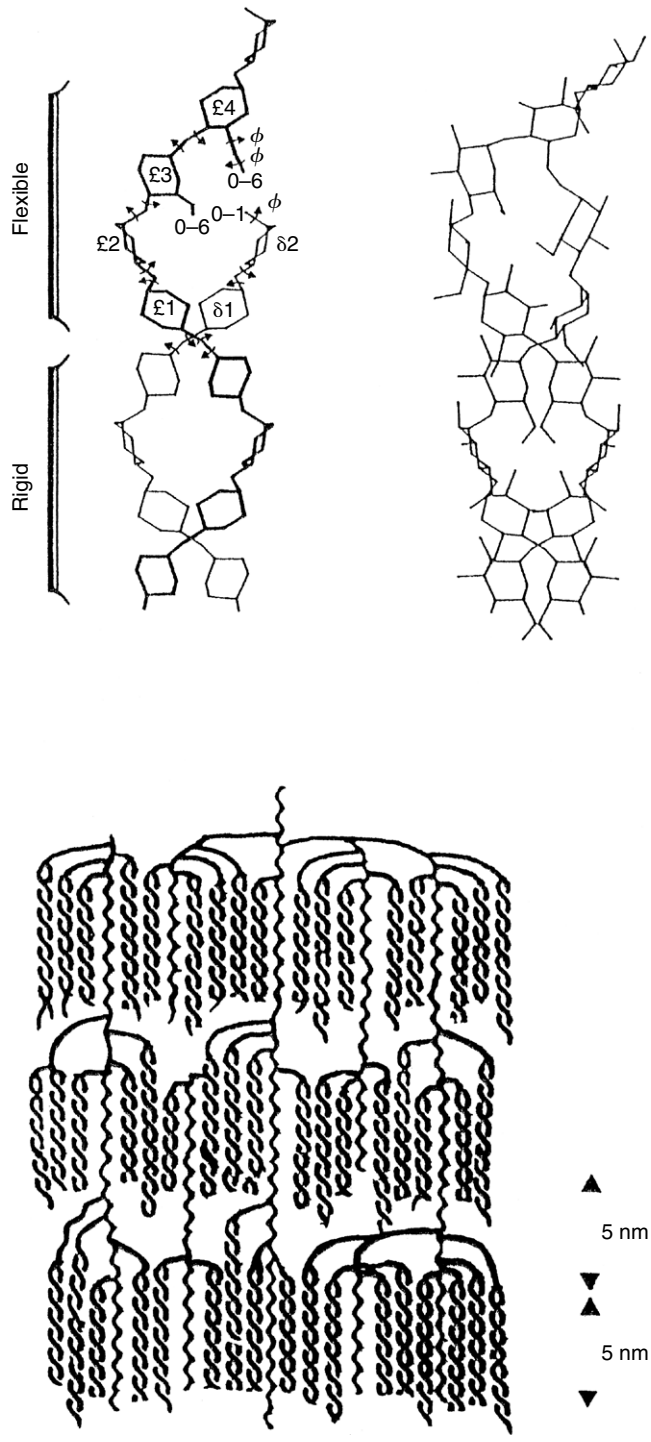

Figure 5.11 Representation of the double helix of crystalline starch after modeling a branching point between two strands. Schematic cluster model of amylopectin molecule incorporating the double helical fragments. (Reproduced with permission from reference 45)

used as building blocks of larger systems.[49] The possible make-up of amylopectin unit clusters was investigated via a series of models, including single–single, double–single, and double–double helix systems. The lengths of the single helix section linking two branch points (internal chains) was systematically varied between values of 0 and 10 glucosyl units. It was found that certain internal chain lengths led to parallel double helices. It can, therefore, be postulated that the length of internal chains may determine the degree of local crystallinity. Furthermore, it was noted that some low-energy arrangements of double helices could be superimposed on either of the two adjacent or non-adjacent double helices of crystalline A and B starch polymorphs (Figure 5.12). In other instances, the distance between the double helices is so large that it may in fact be a model for the branching separating two amylopectin crystals or unit clusters. Results of such a modeling exercise strongly suggest that the branching in amylopectin is not random. This, in a sense, is not a surprising feature, as the branching process is controlled by the specific enzymes involved. The location and the length of branching segments necessarily reflect the three-dimensional structure and specificity of the branching enzymes, along with the spatial and temporal availability of the oligosaccharide complexes involved in synthesis (Chapter 4). It might, therefore, be emphasized that the characteristics of branching pattern are equally as important as chain length distributions, and that they play a determinant role in some physicochemical properties of starch.

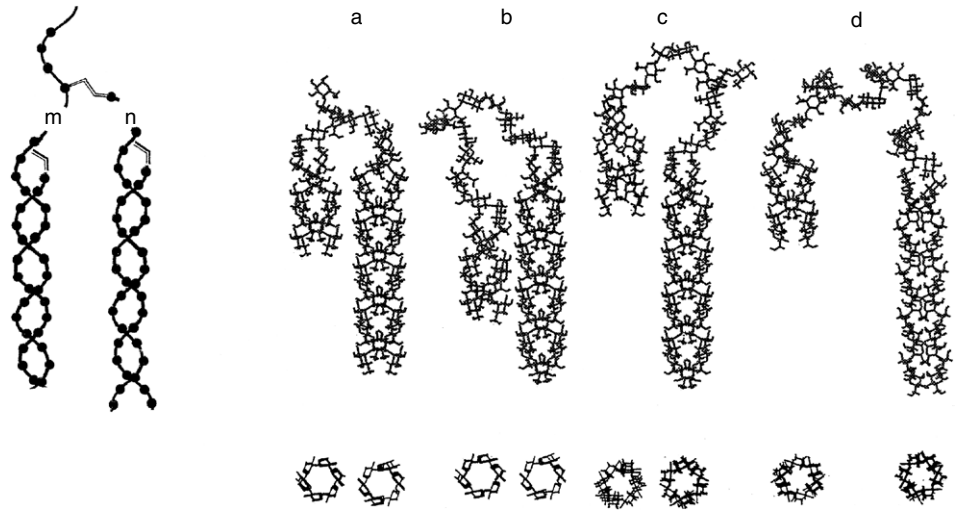

Figure 5.12 Schematic representation showing some parameters underlying branching between two double helices. The number of α-D-Glc*p* units on the reducing side and the non-reducing side of the (1→6) linkage are designated as *n* and *m*, respectively. Molecular drawings of some low-energy arrangements as a function of *m* and *n*: (a) $m = 1$, $n = 3$; (b) $m = 4$, $n = 6$; (c) $m = 6$, $n = 4$; (d) $m = 7$, $n = 7$. The m = 1 and n=3 model (a) is easily superimposed on two adjacent double helices as found in the A allomorph. The $m = 4$ and $n = 6$ model b superimposes equally well on the A- and B-crystalline starch structures. The $m = 6$, $n = 4$ model c corresponds to two non-adjacent double helices of crystalline B-starch. (Reproduced with permission from reference 49)

The domain structure in starch has been investigated by the use of enzyme-catalyzed hydrolysis, followed by either scanning or transmission electron microscopy, with the aim of characterizing the mosaic composition of starch resulting from the presence of 'hard' and 'soft' material.[50] During α-amylolysis, most crystalline (hard) regions are less digested than are semicrystalline (soft) regions (Figure 5.13). Examination of the three-dimensional structure of pig pancreatic α-amylase reveals that the binding site cannot accommodate such large and stiff fragments as the double helices found in the crystalline A- and B-allomorphs[51] (Figure 5.14).

The susceptibility of starch granules to hydrolysis catalyzed by α-amylase can be quantified by following the degree and the manner in which erosion and corrosion take place. Most starch granules are first hydrolyzed superficially. Granules of some

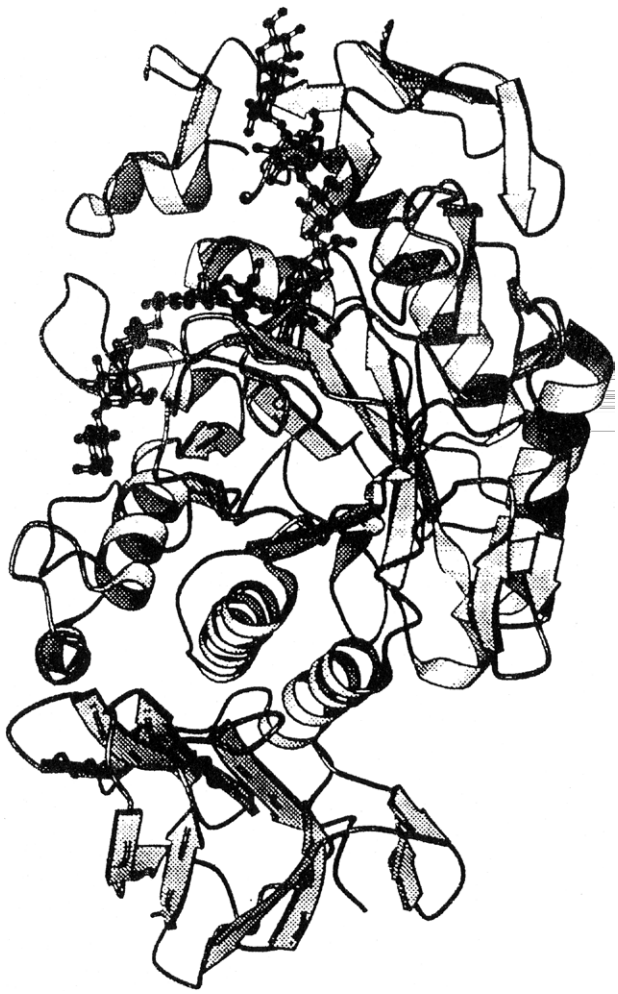

Figure 5.13 Interaction of an amylose chain in the vicinity and in the hydrolytic site of pig pancreatic α-amylase. The impossibility of fitting a double helix in the hydrolytic site has been clearly established, along with determination of the direction of binding of the amylosic substrate in the cleft of the enzyme. (Reproduced with permission from reference 51)

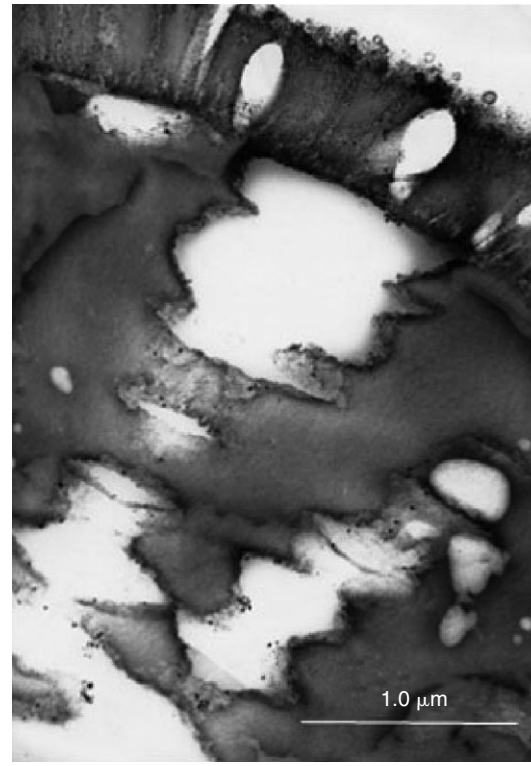

Figure 5.14 Transmission electron micrograph of waxy maize starch granule after α-hydrolysis showing internal canal of corrosion. In the outer shell diameter, the size of the thin canalicles is about 25 nm. (Gallant, unpublished)

starches have specific openings and/or susceptible surface zones, which become enlarged and/or form pits due to endocorrosion. As the pores or pits become larger, canals of endoerrosion sink into the granules.[1,11] In maize starch at least, and probably also in other starches with endogeneous pores and channels, channel openings appear to be enlarged, not only from the outside in, but also from the inside out. Scanning electron microscopy observations at high magnification of starch granules that have been treated by amylases indicate that granules of at least some starches are composed of small (50–500 nm diameter), more or less spherical 'blocklets.'[1,11,52] These blocklet structures are shown in Figure 5.15, and are further discussed with respect to starch granule structure in Sections 5.4 and 5.5.

The super helical structure in starch has been characterized by transmission electron microscopy of small, negatively-stained granule fragments. With proper preparation conditions, the lamella structure is not disrupted.[24] Using results of electron tomography on negatively-stained potato starch granule fragments and cryo-electron diffraction of frozen-hydrated granule fragments, a model for the structural organization of amylopectin in potato starch granules has been proposed.[3] In this model, helices form a continuous, regular crystalline network, which appears to be a framework skeleton around which the rest of the granule is built. The crystalline domains

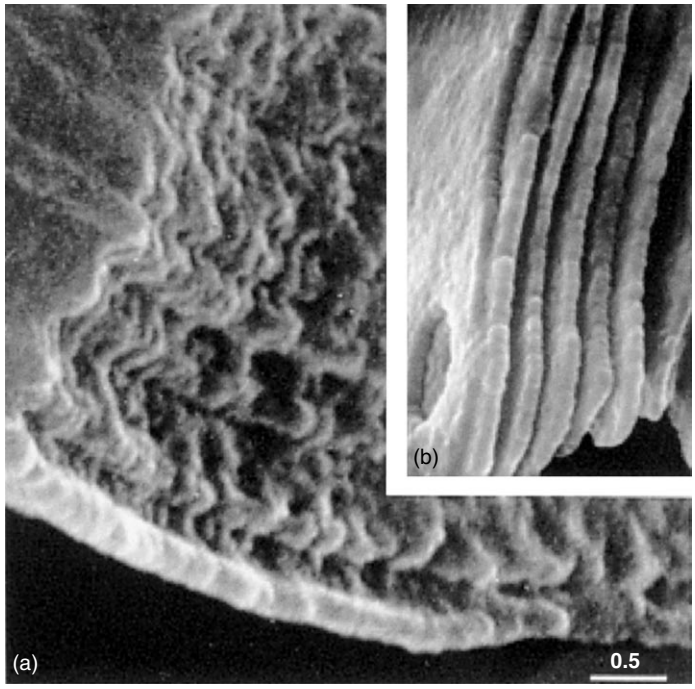

Figure 5.15 Scanning electron micrographs of starch granules after mild α-amylolysis showing the occurrence of spherical blocklet-like structures. (a) potato; and (b) wheat starch granules. (Adapted with permission from reference 1)

containing the double helical linear segments in the amylopectin molecules form a continuous network consisting of left-handed helices packed in a tetragonal array. Since neighboring helices interpenetrate each other, the crystalline lamellae form a more or less continuous superhelical structure. Such a semicrystalline structure is built up from more or less continuous left-handed fragments, and has a diameter of approximately 180 nm and a pitch of 10 nm (Figure 5.16). A central cavity within the super helices would have a diameter of about 8 nm. It is proposed that the pitch of the helix in starch originates from the clustering of branch points and may be characteristic for the botanical source. Helical pitch would therefore be determined directly by the specificity of the branching enzymes involved in the synthesis of amylopectin (Chapter 4).

III. The Granule Surface

Characterization of the state, nature and structure of the starch granule surface has been somewhat limited. Over the past few years, however, substantial progress in starch surface chemical analysis and surface imaging has been made. The following two sections detail recent developments in these two new areas of starch research.

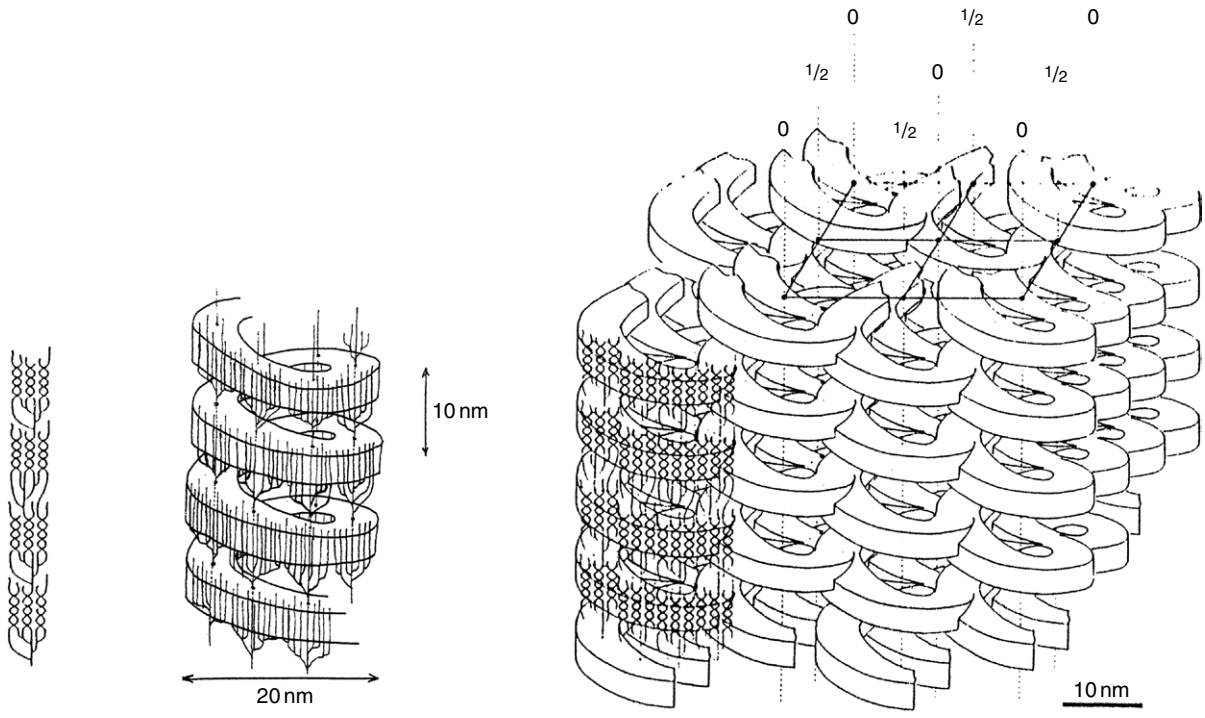

Figure 5.16 Schematic model for the arrangement of amylopectin in potato starch. Crystalline layers containing double helical linear segments in amylopectin molecules form a continuous network consisting of left-handed helices packed in tetragonal arrays. Neighboring molecules are shifted relative to each other by half the helical pitch. (Adapted with permission from reference 3)

1. Starch Granule Surface and Chemistry and Composition

For most starches, the external surface of starch granules is the first barrier to processes such as granule hydration, enzyme attack and chemical reaction with modifying agents. Consequently, it is becoming recognized that the nature of the granule surface, and particularly the presence of surface proteins and lipids, may have significant effects on the properties of the starch.[53–58] For example, the presence of lipids at the granule surface appears to influence the rheological properties of starch–water pastes,[57] and changes to both the protein and lipid at the granule surface are implicated in the improved baking performance of chlorine-treated flour.[54,56,58,59]

Starch granule-associated protein and lipid are by far the most abundant of the minor components of starch.[60,61] These components are thought to be incorporated into the granule during its synthesis, although in a cereal starch sample which has not been well washed, some protein from the endosperm may adhere to the granule. The true granule-associated proteins are distinct from the endosperm (gluten) proteins and many are believed to be enzymes which were involved in granule synthesis (hence, such proteins are found even in tuber starches).[60,62] The exact origin of the true starch lipids is not fully known, although it has been hypothesized that free fatty acids and lysophospholipids are normal membrane degradation products that are rendered metabolically inactive by incorporation in the granule (i.e. complexation with

amylose – see below).[61] Furthermore, it has been hypothesized that some lipids may have a direct role in the function of granule-bound enzymes, and that lipo-protein complexes may exist.

The exact quantity of protein and lipid present depends on the species and variety of starch; however, typical well washed cereal starch samples contain ~0.3% protein and up to 1.0% lipid, while a typical root or tuber starch may contain ~0.05% protein and 0.05–0.1% lipid.[63] These values result from bulk analysis of starch; in reality, the actual distribution of the components is not uniform, with both protein and lipid enrichment believed to be present towards and at the granule surface.[58,64,65]

2. Surface-Specific Chemical Analysis

To date, surface-specific analysis of the starch granule has been limited. Until recently, the only substantial work in this field was the XPS (x-ray photoelectron spectroscopy) study of native and chlorine-treated starch granules performed in 1987 by Russell et al.[66] Recently, however, substantial surface specific analysis of a range of native starch granules has been performed using the complementary techniques of XPS[58] and time-of-flight secondary-ion mass spectrometry (TOF-SIMS).[67] The semi-quantitative TOF-SIMS study allowed extensive characterization of the various carbohydrates and lipid species found in the outer 1–2 nm of native (and chlorine-treated) wheat, rice and potato starch granules.[67] Peaks assigned to carbohydrate structures included a series of peaks (at m/z 221-, 383-, 545-, 707-, 869- and 1031-) corresponding to dimers, trimers, etc. of the basic glucosyl monomer unit and a peak at m/z 405- which corresponds to a dimer with one ionic phosphate group attached (at either the O-1, O-3 or O-6 position) (O-1 should, however, be excluded). Characterization of the lipid peaks identified the free fatty acids, glycerides and phosphoglycerides at the surface of each sample, including precise determination of their hydrocarbon chains. The presence of nitrogen-containing species was also evidenced, and attributed to peptide fragments, although the precise identification of peptide species was not possible with the instrument used. The complementary quantitative XPS study of native (and chlorine-treated) starch granule surfaces allowed the elemental composition of the outer 5–10 nm of the granule surface to be reproducibly and accurately determined. The results, which have yet to be fully published, build on and confirm the study by Russell et al.,[66] and lend considerable weight to the view that substantially higher levels of protein and lipid are found at or near the surface of the granule.[58] Mathematical modeling from the elemental percentages provided by XPS experiments suggests that the bulk (~90% in cereal starches and ~95% in potato starch) of the granule surface is carbohydrate in nature.[58] Granule surface protein was found to represent around 5% of the cereal starch surface and 0.05% of the potato starch surface. Both starch types may have up to 5% lipid at granule surfaces.[58]

Initial progress in characterizing and understanding the surface chemistry of starch granules has thus been made. In association with such chemical characterization, significant advances in the investigation of the structure of the starch granule surface have also been made, due to recent advances in surface imaging techniques.

IV. Granule Surface Imaging

Since the early 1990s, surface imaging has rapidly and extensively advanced, due to the development of a wide range of scanning probe microscopy (SPM) techniques.[68] The development of the atomic force microscope (AFM) in 1986,[69] which stemmed from the invention of the scanning tunneling microscope (STM), revolutionized the field by permitting molecular and even atomic resolution imaging of non-electrically conducting samples. The technique allows samples to be imaged under ambient conditions, either in air or under liquids, and usually requires minimal sample preparation compared to other forms of microscopy. Furthermore, a range of AFM modes and derivative techniques exist,[68,70] allowing mapping of the mechanical and chemical properties of the sample, as well as producing images. Consequently, prospects of imaging under virtually 'native' conditions at superior resolution to that obtained using current scanning electron microscopy (SEM) techniques has sparked substantial interest in AFM imaging of non-electrically conducting biological samples, such as plant cell walls, polysaccharide gel networks and living cells.[70–76] Applications of AFM imaging to starch research have been limited in number,[58,59,75,76] but they have successfully demonstrated the potential of the AFM technique in starch research by revealing important new insights into starch granule structure, molecular organization and degradation kinetics. This section aims to demonstrate the significant advantages that AFM imaging of starch offers over SEM imaging, and to highlight the important future role of the AFM technique in furthering understanding of both starch granule architecture and its component polysaccharide polymers.

1. Granule Imaging by SEM Methods

Until the 1990s, research aimed at imaging starch granule surfaces was largely limited to conventional scanning electron microscopy (SEM). Starch granules are not, however, ideal specimens for SEM imaging, due to their particulate, biological, non-electrically conducting nature. Thus, while SEM has proved to be (and continues to be) invaluable in increasing our knowledge of the starch granule surface, internal structure, patterns of enzyme attack and transformations,[11,78–85] it can rarely be used to its full potential with biological samples (in terms of image resolution), due to charging and subsequent damage of the electrically insulating starch granules. Furthermore, samples for conventional SEM can never be imaged in their original state, since the imaging is performed in a high vacuum and techniques of preparation associated with it may change the structure of the products and introduce undesirable artifacts.

Environmental scanning electron microscopes (ESEM) are new variable pressure SEMs working at moderate vacuum in the sample chamber (in the range of 1 to 50 Torr) while the electron column is maintained under high vacuum.[86,87] This SEM provides imaging capabilities with uncoated dry, moist or oily samples, thus reducing the risks of damaging samples as well as creating artifacts. Létang et al.[87] studied bread dough at different water contents (50–56% moisture). McDonough and Rooney[88] observed that the starch granules in a fully-hydrated wheat starch–water dough appeared rounder and plumper than when viewed with conventional SEM

under high vacuum. Fannon et al.[84] used ESEM in order to investigate specific surface openings of some starch granules, with samples being examined wet or dry in a water vapor environment of 2–10 Torr. However, ESEM experiments have not been extensively developed for, or applied to, starchy products; even structural studies of the behavior of starch granules during hydrothermic processing and enzyme treatments could be exploited using this technique.

Using conventional SEM methods, drying or freezing (cryo-SEM) is employed to either dehydrate the samples or fix the water phase temporarily as a solid. In order to achieve high-quality images of starch, the specimen has to be metal-coated (e.g. with gold or platinum) to avoid sample charging and to improve the secondary electron signal strength (although it is still notoriously difficult to obtain quality high-resolution images of starch granule surfaces, even after coating).

Used in order to follow the behavior of starchy components during thermal processing (water uptake, granule swelling, leaching of amylose, retrogradation) cryo-SEM has revealed structural features not seen by classic cyto-techniques.[89] Some of the highest resolution images of starch granules were acquired in the 1970s using an SEM instrument capable of working with extremely low beam currents (1×10^{13}A).[1,50,90,91] High-resolution images of gold-coated (dried), α-amylase-attacked starch granules were achieved, revealing information about granule internal structure (see below).[79,81,92,93] Low-voltage scanning electron microscopes (LVSEM) also offer considerable advantages over conventional SEMs for imaging of biological samples, because the primary electron beam in a LVSEM is generated via field emission rather than by thermo-ionic emission. Therefore, such instruments are capable of achieving high-quality images (resolutions of a few nanometers are quoted for modern instruments) at very low accelerating voltages (e.g. 500 V).[94] The technique is still performed in a vacuum, but sample charging and damage are considerably reduced, permitting most electrically insulating samples to image without coating. This is of advantage in high-resolution studies, since the thin metallic surface coats required by conventional SEM are particulate in nature (particle size can be up to 10 nm) and hence, there is a potential problem of misinterpretation of results at high resolution.[74] LVSEM has been extensively applied for imaging of a range of insulating biological specimens,[94–96] but its application to starch granule imaging has been limited. However, the usefulness of this technique for providing superior images of native uncoated starch granule surfaces, as compared to other forms of SEM, which complement and validate higher resolution AFM studies, has been demonstrated.[59,60,97]

2. Principles of AFM

Detailed technical descriptions of the AFM technique, also known as scanning force microscopy (SFM), can be found elsewhere.[69,98,99] In brief, AFM is a lens-less microscopy technique in which a sample surface is brought into such close proximity with a fine crystal tip mounted on a flexible cantilever that atomic interaction forces between the tip and the sample cause the cantilever to bend. Bending of the cantilever in the z (height) plane is monitored and, by scanning the tip across the sample, a three-dimensional image of the sample surface topology is acquired (Figure 5.17). The AFM

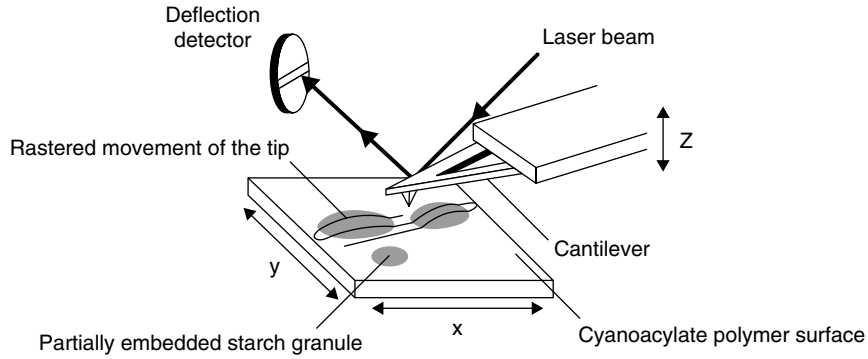

Figure 5.17 Schematic diagram representing AFM imaging of partially-embedded starch granules.

instrument is capable of molecular or even atomic resolution on appropriate samples, with vertical resolutions in the region of 1–2 Å (0.1–0.2 nm) and lateral resolution of 10 Å (1 nm) or less.[75] It is widely recognized, however, that 'soft' biological materials, such as organic molecules, generally are problematic with respect to higher resolutions.[72,100] In support of this, Weihs et al.[101] have speculated that the limit of imaging resolution of 'soft' (e.g. biological) samples may be 2–3 nm (20–30 Å) at best with small forces applied in air. Nevertheless, it is clear that such resolution coupled with the minimal need for uncoated sample preparation, the ability to image in a range of environments (ambient, air, liquid, cryo, heated), and the extensive range of imaging AFM modes offers opportunities for further investigation of starch granules.

3. Sample Preparation for AFM Imaging of Granular Starch

Sample preparation for AFM imaging is critical for achieving reproducible, high-quality and meaningful results. Although routine methods have been reported for preparation of isolated polysaccharide chains on flat supports,[70] AFM imaging of starch granules (particles that have diameters in the range of ~0.1 to 200 μm) presents a number of problems directly connected with the size and morphology of the samples. In particular, these problems merge with curved or dotted surfaces, or when special methods for material preparation are required in order to expose the bare inner surface of the starch granule.

Ideally, AFM should be performed on flat surfaces, due to the need to raster the cantilever across the sample at a micrometric scale, and because large sample height differences (greater than a few micrometers) may either prevent tip scanning, due to the limits of the vertical motion of the cantilever or cause 'self-imaging' of the tip, due to the sides of the tip becoming involved in image generation,[100,102,103] Non-fixed particles may also suffer problems of probe-induced particle movement or 'sweeping' as the probe moves across the sample.[103] It is for these reasons that almost all published AFM studies of whole starch granules[59,67,77,105] have involved embedding of the granules in order to immobilize them, and to reduce the overall height variation of the sample surface. It was reported[106] that physical destruction using a glass

homogenizer was more suitable for observation of the bare inner surfaces of the starch granules than was using digestion or cutting, but the new tendency is to study thin sections of granules encased in resins using the contact mode.[107–110]

4. Surface Detail and Inner Granule Structure Revealed by AFM

Using suitable preparation techniques, reproducible AFM imaging of starch granules has been performed. While studies performed to date had different aims and resulted in images of the starch granules at different resolutions, they are complementary in nature and demonstrate both the versatility and applicability of the AFM technique to starch research. It is, nevertheless, important to recognize the primary sources of artifacts in AFM images.[104,111]

Real-Time AFM Studies of Degradation by Enzymes

The AFM study of wheat starch granules from the cultivar Timmo by Thomson et al.[77] is the earliest recorded usage of AFM to image the starch granule surface. The aim of the study was to demonstrate the potential of the AFM technique to image a biological process in real-time, using starch granule digestion by α-amylase as the example system. From images of the granules taken in air (before introduction of an aqueous solution), Thomson et al.[77] reported that the surface of the starch granule appeared to be 'dotted with features between 50 and 450 nm across,' and that a highly elongated structure was seen on the surface of a granule in one image. No explanation of the 50 to 450 nm structures was given, but they postulated that the elongated structure may have been a contaminant, possibly a protein molecule. Some granules were reported to have 'cracked' surfaces, and it was postulated that this may have arisen from milling of the wheat kernels during extraction of the flour. On introduction of the enzyme solution (after any swelling had finished), the surface of the granules appeared to become covered by the enzyme rapidly, although the binding appeared to be weak, since the enzyme was easily displaced by the AFM tip. They then followed the attack of the starch granules by enzyme molecules by recording images at 105-second intervals. The granule appeared to be attack by α-amylase preferentially (and rapidly) at sites of damage (i.e. weak spots) via the classic 'pinhole' attack pattern.[1] A pile-up of material seen at the edge of the hole was attributed to possible interference of the tip in the hole formation. As the hole became deeper, the shape of the hole appeared to become square, due to the inability of the pyramidal AFM tip to accurately image inside the hole, i.e. the square shape of the hole reflects that of the AFM tip.

High-Resolution AFM (and LVSEM) Studies of Starch Granule Surface Structure

In parallel with the surface-specific chemical analysis of the native starch granule surface (detailed above), high-resolution imaging of native starch granule surfaces was performed using both LVSEM and AFM.[58,59,97] The aim was to visualize at high-resolution the surface structure of native starch granules with known differences in granule size, structure and minor components.

Observation of potato starch granule surfaces: in general, in LVSEM images (Figure 5.18a), the potato starch granule surface had a rough, undulating appearance with occasional indentations and numerous small, raised nodules that were approximately 100 to 300 nm in diameter (evident as small bright areas). The roughness of the surface can be clearly seen in the images (Figure 5.19a), where the presence of the small raised nodules (approximately 50 to 300 nm in diameter) is highly apparent. Higher-resolution images[97] indicate that the raised nodules appear to protrude above a smoother surface which consists of smaller semi-spherical structures (~20–50 nm in diameter). Large surface 'blebs' (gross surface 'lumps' occurring mainly at the 'poles' of a granule,[112] occasionally evident on some potato starch granules), have been imaged by both LVSEM and AFM.[104]

Observation of wheat starch granule surfaces: in comparison with the potato starch surface, the surface of both a and b wheat starch granules appeared to be relatively smooth (Figure 5.18b), possessing only a few surface blemishes and an occasional raised nodule. From the corresponding AFM images (Figure 5.19b), it is evident that the wheat starch granule surface appears to consist of a mass of similarly-sized structures (20–50 nm in diameter). Some larger structures (50–300 nm in diameter) corresponding to the raised nodules of the potato starch are present, although their

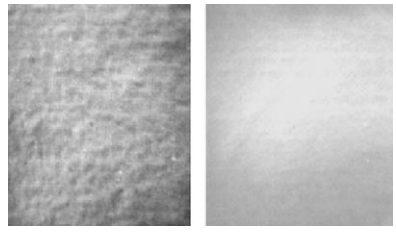

Figure 5.18 (a) LVSEM micrograph of a typical potato starch granule surface region (magnification 10000×, scale bar represents 3 μm); (b) LVSEM micrograph of a typical region of a Riband wheat starch granule surface. (Magnification 10000×, scale bar represents 3 μm)

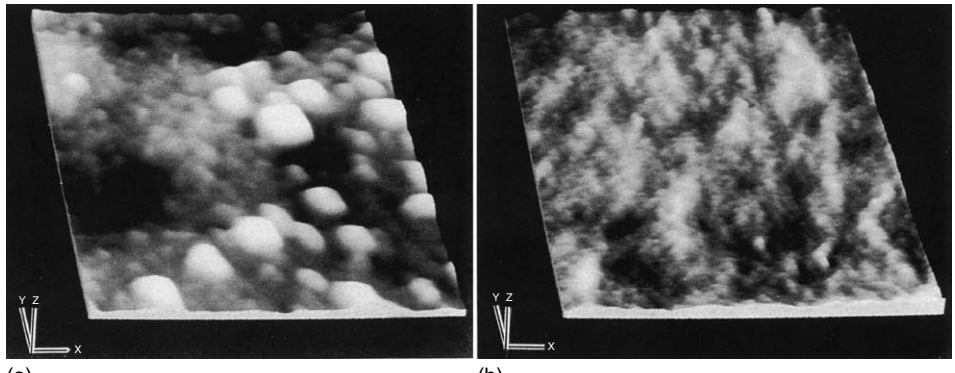

Figure 5.19 (a) AFM image of a typical surface region of a potato starch granule (scan size 1000 nm^2, z height difference 73.8 nm); (b) AFM image of a typical surface region of a Riband wheat starch granule (scan size 1000 nm^2, z height difference 52.6 nm)

occurrence is far less frequent than on potato starch granules. The same observations were reported for barley, oat, maize, waxy maize and triticale granules.[113,114]

Another method used for starch is the non-contact mode, where the starch granules are simply spread onto an adhesive tape fixed on the AFM sample holder. Using this technique, both nodules (20–50 nm in diameter) and smooth areas without any visible features were observed at the surface of potato starch granules.[114] Multiple freeze–thaw cycles have revealed an internal, lamellar structure of chain clusters bundled into 'blocklets' 50–300 nm in diameter.[115]

Observation of inner structures of starch granules: as noticed by Ohtani et al.[106] AFM, which gives greater resolution as compared with electron microscopy, needs very precise tools. In particular, the amplitude mode image may be used to enhance edge contrast of samples, but resolution of the probe remains limited by the radius of the crystal tip and its finite thickness. This very important point and the choice of method of sample preparation are the main limiting factors for imaging accuracy. AFM images in the tapping mode obtained from starch granules from different botanical sources[106] showed no large size aggregates but, in all cases, similar small particles of approximately 30 nm in diameter, often arranged in straight, chain-like structures. Particularly visible on the AFM images of crushed sweet potato starch granules, such chains appeared bundled into rods or larger columns. Similarly, ring-like protrusions were seen (non-contact mode) in potato starch granules frozen in excess water, then dried.[116] These structures were interpreted as individual 'blocklets' or single clusters, because their size was comparable to that of 'blocklets.'

5. Interpretation of AFM Images with Respect to Granule Structure

Observation of two starch types by AFM and LVSEM demonstrates that, on a macromolecular scale, the surfaces of starch granules differ, i.e. there are significant differences in granule surfaces between starches from different botanical sources. Observation of the raised nodules (50–300 nm in diameter) on granule surfaces of granules corresponds well with the observation of Thompson et al.[77] of 'features between 50 and 450 nm across,' although the structures are thought to be carbohydrate in nature.[97] This deduction arises from the facts that: (a) the features are far more common on potato starch granule surfaces than on the surfaces of wheat starch granules (the surface protein content of potato starch granules is much less than that of wheat starch granules); and (b) protein molecules are far smaller than the 50 to 300 nm structures, e.g. one hemoglobin molecule which has a molecular weight of ~66 kD (similar to starch granule-bound starch synthase SGBSSI) has a diameter of only 5.5 nm. Thus, extremely large numbers of protein molecules (e.g. multi-molecular complexes) would have to be present to explain the quantity and size of the structures seen on the surface of potato starch granules by AFM. Such a quantity of protein does not, however, fit with the observation that ~95% of the granule surface is carbohydrate in nature. Moreover, potato starch granules (which have far more of the raised nodules than do wheat starch granules) have only ~0.05% surface protein (i.e. about tenfold less protein than does wheat starch).[58]

Observations regarding the surface structure of potato and wheat starch granules in the AFM study of Baldwin et al.[58,59,97] support the SEM observations of Gallant et al.[1,11,50] who described the structure of starch as being composed of 'more or less spherical blocklets,' which were observed both within and at the surface of starch granules degraded by α-amylase. In general, the 'blocklets' were found to be larger (400–500 nm in diameter) in starches of the B- (e.g. potato starch) and C-crystalline types than in starches with the A-crystalline type (e.g. wheat starch, in which the blocklets were 25–100 nm in diameter). Full discussion of the findings with respect to current (and historic) views on the structure of starch granules has been made;[11] they are further presented in Section 5.5. However, in brief, it was shown that, in wheat starches, larger blocklets (100 nm) are found in the hard crystalline 'shells' of the granule than in the softer amorphous shells (blocklet size is ~25 nm in the amorphous shells). In potato starch, very large (400–500 nm) blocklets are found in the outer 10 μm of the granule, with smaller blocklets towards the granule center. Such observations (in association with other isolated evidence in the literature; see Section 5.5) have demonstrated the real presence of a blocklet structure in starch, and have led to the hypothesis that large blocklet size contributes to starch resistance due to locally increased levels of crystalline structure.[11] Observation of this crystalline blocklet structure in starch granules leads to obvious questions as to whether the blocklets represent single molecules of amylopectin, and if so, whether the different-sized blocklets represent molecules of amylopectin with different molecular weights and/or different degrees of branching. Currently, such questions cannot be definitely answered from data and images available. However, Martin and Smith[117] stated that the average diameter of an amylopectin molecule is 200 to 400 nm, and that such a molecule would contain 20 to 40 side chain clusters. It is, therefore, clear that these average dimensions for the amylopectin molecule are congruent with the average size of the raised nodule (blocklets) seen at the surface of, and within, starch granules as investigated by AFM[106] and SEM.[1,11,50] Furthermore, from published values relating to the size of a glucosyl unit and to the size of amylopectin side chain clusters, it is possible to estimate the number of glucosyl units and amylopectin side chain clusters present in the raised nodule (blocklet) structures. Firstly, since the diameter of a glucosyl unit has been estimated to be approximately 0.4 nm,[2] it is evident that a raised nodule structure with a diameter of 20 nm could contain an absolute maximum of 50 glucosyl units across its diameter (if they were placed directly adjacent to one another). The glucosyl units are not, however, side-by-side, but arranged into A- and B-type crystalline lattices, as demonstrated by computer modeling simulations of the starch polymers.[118] The computer models were based on amylose chains; however, the crystalline arrangements are thought to be relevant to the side chains (A- and B-chains) of amylopectin molecules which form crystalline clusters. As previously stated, the clusters are alternatively grouped with the branching regions of the amylopectin to form layers of crystalline and amorphous lamellae.[16] The average diameter of an amylopectin side chain cluster has been estimated to be 10 nm.[16] It therefore follows, that the smallest structures seen at the surface of starch granules by AFM, which are ~10 nm in diameter, can be attributed to a single amylopectin side chain cluster, and that the slightly larger structures (or blocklets, 20–50 nm in diameter) are on average composed of between 2 and

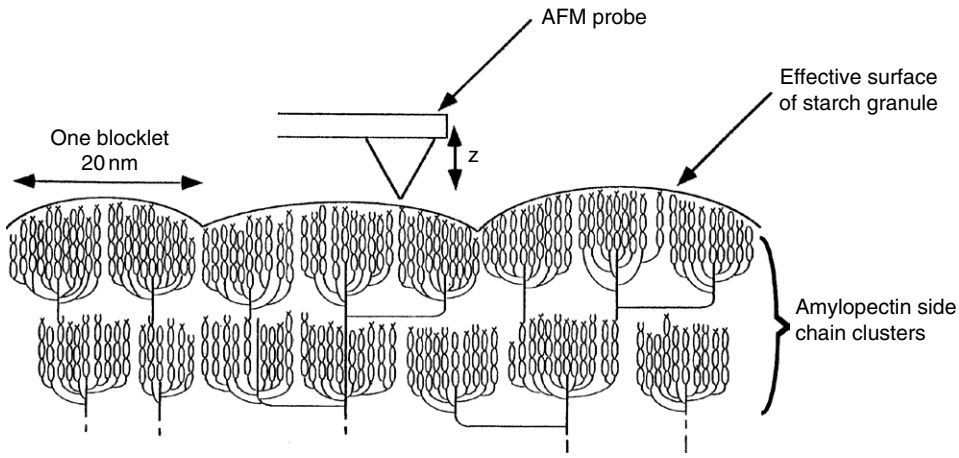

Figure 5.20 Schematic diagram of amylopectin side chain clusters forming the 10–50 nm raised nodule ('blocklet') structures seen at the starch granule surface.

5 amylopectin side chain clusters. The substantially larger blocklets (50 to 500 nm in diameter) would therefore contain between 5 and 50 amylopectin side chain clusters. On this basis, it has been postulated[97] that the structures revealed in the AFM images are amylopectin side chain clusters grouped into blocklets seen from above (Figure 5.20), and that the near-molecular resolution of potato and wheat starch granule surfaces has, therefore, been achieved by AFM imaging.

6. Discussion of Granule Surface Imaging by Scanning Probe Microscopy (SPM)

Representative Sampling and Imaging Artifacts

Due to the very nature of the high-resolution imaging provided by AFM, the total sampling area in AFM studies is inherently very low. Consequently, it is highly important to ensure that sample representivity is achieved in the resulting images. As detailed above, low-voltage (field-emission) SEM can be viewed as a complementary technique to AFM, due to its applicability to biological samples after minimal sample preparation and its ability to provide high-resolution images of uncoated samples. The technique facilitates imaging of comparatively large areas on numerous samples, and provides images that normally have sufficiently high resolution to allow confirmation of the AFM images. Furthermore, the technique provides a prior knowledge of the sample at high resolution, thus giving extra security in ensuring correct interpretation of subsequent AFM images. This is evident in the study of Baldwin et al.,[97] where there is clearly a high correlation between the AFM and LVSEM images with respect to granule surface topology of the two starch types, allowing the conclusion that subsequent AFM images are representative.

While the use of a separate LVSEM instrument to ensure sampling representivity provides high-resolution imaging of uncoated samples, various other approaches also exist. For example, there are now scanning probe microscopes located within

scanning electron microscopes[119] and AFM instruments which attach to inverted optical microscopes.[68] These systems allow SEM imaging of large surface areas (e.g. 1 cm^2), followed by 'zooming-in' to analyze the area by SPM. Thus, not only is exactly the same sample imaged by both techniques, thereby providing a full range of resolutions, but the state of the SPM tip can be regularly checked by SEM. Clearly, however, SPM imaging in such instruments is performed in a vacuum, and the use of conventional SEM requires biological samples to be metal-coated. The use of a combined LVSEM/AFM instrument would, however, be of interest for biological samples.

Instruments in which an AFM head is attached to an inverted optical microscope offer optical and SPM imaging of the same biological samples in a range of environmental conditions, and are particularly powerful when coupled to a high-resolution optical microscope such as a confocal laser scanning microscope (CLSM). Complementary images of samples can thus be obtained at a range of resolutions to ensure representivity (and correct AFM positioning). The images may also contain some chemical information, due to the feasibility of fluorescence optical imaging and some internal structural detail of the sample, due to the optical sectioning ability of the CLSM.

AFM Imaging Mode, Imaging Environment and Improving Resolution

In general, non-contact or tapping-mode AFM is recommended for biological specimens,[74,120] since these modes reduce the potentially damaging forces (both lateral and vertical) experienced by the sample due to the close proximity of the AFM probe. This advice holds for small, easily-displaced biological samples (e.g. individual molecules) and for soft, easily-deformed biological samples (e.g. viscous liquids and living animal cells), but experience has shown that non-contact or tapping-mode AFM is not necessarily required for high-resolution imaging of whole, native starch granules. At ambient conditions (~22°C, ~10% water content) starch granules are below their glass transition point[121] and are, therefore, comparatively rigid and robust compared to other biological specimens (e.g. live cells). The AFM examinations detailed above demonstrate that the constant-force, contact-mode of AFM in air (and in an aqueous environment) can be successfully employed for imaging of partially-embedded starch granules, without the generation of gross imaging artifacts.

The AFM imaging environment chosen is often governed by the type of experiment required. As stated above, AFM is unique in its ability to offer high-resolution imaging under a variety of imaging environments, e.g. gas, vacuum, liquid (aqueous or non-aqueous). Thomson et al.[77] demonstrated imaging of starch granules in air and in an aqueous environment. Baldwin et al.[97] acquired high-resolution images of starch granule surfaces in air. This choice was made because a starch granule surface under ambient conditions in air was deemed to be in as 'native' a state as possible, but it is possible that even higher-resolution imaging of starch granules is possible if imaging is performed under other conditions. This is because any moisture in the air has a tendency to condense onto both the sample surface and the AFM tip. Capillary action between the tip and the surface may then cause large attractive forces between the two in the order of 10^{-6} to 10^{-8} N, which tends to increase the chances of sample damage and decrease image resolution.[70,122] Consequently, imaging of biological

samples, particularly 'soft' samples or isolated molecules, is often performed under an alcohol (e.g. 1-butanol), where problems of water absorption are not experienced, hence permitting imaging with smaller, less damaging contact forces.[70,123] Whole starch granules appear to be relatively robust, thus allowing comparatively high-resolution imaging in air without significant sample damage, but imaging under alcohol might be considered in future work as a means of achieving higher resolution. Similarly, there is increasing interest in the imaging of biological samples in vacuum, as suggested in the original AFM paper of Binnig et al.[69] Although imaging in vacuum may cause potentially damaging sample dehydration, image resolution is often improved, due to the reduction in contact forces obtainable under such conditions.

So far, AFM imaging of starch granules has only been performed with pyramidal Si_3N_4 tips. While these tips are standard, high-quality tips, other types of tips exist which, due to their higher aspect ratios, can generally be used to acquire higher-resolution images than those obtained with the standard Si_3N_4 tips. The properties of most commonly available AFM tips (as well as most common AFM imaging artifacts) have been extensively reviewed.[102,104] In general, it is held that by reducing the diameter at the tip of the probe, image resolution is improved, due to reduction in interaction forces between the sample and the probe tip.[101,102] However, very thin tips are more easily damaged, and the risk of damaging the sample increases as tips are sharpened.[100] Clearly, therefore, in achieving higher resolution imaging of starch, the choices of tips, imaging mode and imaging environment need to be optimized. However, the use of higher aspect tips, in non-contact/tapping mode, in air or under alcohol, would seem to represent logical steps in the right direction.

7. Future Prospects of SPM of Starch

The preceding sections demonstrate that scanning-probe microscopy of starch is in its infancy. The few SPM studies performed to date, however, demonstrate the potential of AFM for observing the starch granules at high resolution under a range of conditions, and it is evident that it is becoming possible to observe structures which previously could only be investigated by x-ray scattering techniques. To date, however, except for a few cases, AFM imaging of starch has been limited to contact-mode imaging in air. Under such conditions, AFM imaging of 'soft' biological samples has been predicted to have an imaging resolution limit of 2–3 nm at best, in spite of the improved method of image acquisition known as 'AFM by error signal image,' which considerably enhances the high spatial frequencies and sharpens the contrast of features. Starch granules are not typical soft biological samples, and hence, it seems probable that by employing the best imaging conditions (as outlined above) this limit may be surpassed. Furthermore, the origin of image contrast in AFM was recently identified.[109,124] A comparative study of sectioned pea starch granules, either embedded in a non-penetrating matrix of rapid set Araldite or in a hydrophilic melamine resin before sectioning, with sections submitted to hydration during sample preparation, showed that, in contact mode images, contrast is introduced and enhanced by swelling of softer and easier to compress hydrated material. Consequently, structural features are visible

in higher resolution AFM images, because the procedure highlights amorphous versus crystalline materials. Nevertheless, it is clear that an image resolution of 2–3 nm, coupled with the minimal need for sample preparation and the ability to image in a range of environments (ambient, air, liquid, cryo, vacuum) offers considerable scope for further AFM investigation of both starch granule surface topology and internal structure.

V. A Hypothesis of Starch Granule Structure: The Blocklets Concept

As stated above, AFM microscopy of starch is in its infancy; however, in either the contact or the non-contact mode, results on the whole provide substantial support of earlier SEM observations and suggest that a level of crystalline structure between that of the large 'growth' rings and the amylopectin lamellae exists in starch granules. There is however, substantial other evidence (both from microscopy and non-microscopy techniques) in favor of such a level of granule structure, which has been termed the 'blocklet level of structure.'[11] This section details this evidence and presents the current re-emergence of the 'blocklet concept' of starch granule structure.

The idea of crystalline units in starch is not new, and can be originally traced back to the prescience of Nägeli,[125] although it was Badenhuizen[126] who first demonstrated the presence of natural resistant units of material in chemically degraded starch. Badenhuizen described these resistant blocks as 'blökchen Strüktur,' from which the term 'blocklet concept' is derived. At the same time, a fibrillar concept of starch granule structure was developed[127,128] and continued, even though it was proven that features supposed to be fibrillar structures at the TEM scale were artifacts.[129] It now appears, however, that both concepts of granule structure (the blocklet and the fibrillar) were in fact founded in truth, with the fibrillar concept being somewhat related to the radial organization of the starch polymers, while the blocklet concept relates to a higher order of crystalline organization within granules.

While SEM[1,11,50] and AFM[58,97,106–108,113–116,124,130,131] images provide strong visual evidence for a blocklet structure of starch, a considerable amount of other supporting evidence from electron microscopy and enzyme treatments exists. Helbert and Chanzy,[132] using hydrophilic melamine resin for preparation of ultra-thin starch granule sections for transmission electron microscopy (TEM), also obtained images in which the outline of individual blocklets with dimensions of a few hundred nanometers were seen. Such structures have been imaged at higher resolution in sectioned corn starch granules contrasted with periodic acid (thiosemicarbazide) silver (PATAg). At a very low degree of oxidation,[50,133] the PATAg marker, which penetrates and thus highlights only the amorphous regions of the granule, revealed the presence of roughly ellipsoidal regions of 20 to 500 nm in diameter, which were less easily penetrated by the marker (silver ions) that corresponded to roughly spherical crystalline blocklets within the granule.[11] Furthermore, the high resolution of the TEM revealed evidence of alternating crystalline and semi-amorphous amylopectin lamellae within the blocklets.[11]

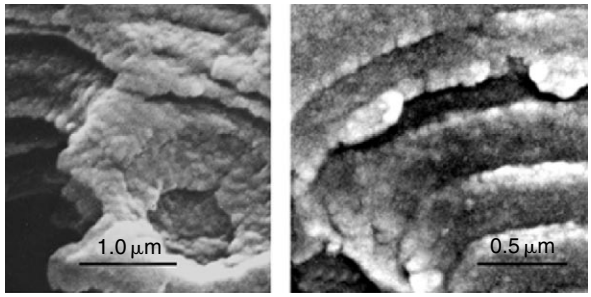

Figure 5.21 Scanning electron micrographs of maize starch granules after α-amylolysis showing resistant shells composed of blocklet-like structures: (a) at internal canal of corrosion level; and (b) at shells level. (Gallant, unpublished)

Further evidence of an intermediate level of granule structure is evident from a number of enzymic degradation studies of starch (Figure 5.21). Bertoft[134] found that the molecules of amylopectin from large and small barley starch granules and from waxy maize starch granules are composed of 'super-clusters' with molecular weights of approximately 10^5. These he interpreted as arising from 'highly ordered regions of amylopectin.' Furthermore, specific (1→4)-α-D-glucosidic linkages between the super-clusters appeared to undergo preferential degradation during initial stages of α-amylolysis, thus releasing the super-clusters. Such observations fit with the idea that an extra level of amylopectin crystallization exists in starch granules, and it has been hypothesized by Gallant et al.[11] that the super-clusters relate to the blocklet structure of starch. The preferentially degraded (1→4)-α-D-glycosidic linkages between the super-clusters must, therefore, be located in the more amorphous 'channel' regions between the blocklets and, thus, are more readily accessible to degradation.

Other approaches to structural determination of starch have been performed by Yamaguchi et al.,[20] by Kassenbeck,[25,135] and by Oostergetel and van Bruggen.[3,24] Yamaguchi et al.[20] used negative staining of crushed, lintnerized starch granules and described 'worm-like ripple structures' in maize starch granules, which they interpreted as 5-nm thick, crystalline lamellae created by association of double helices perpendicular to the plane of the lamellae. Oostergetel and van Bruggen, using a more sophisticated procedure, studied lintnerized wheat[24] and potato starch[3] granules. Three-dimensional reconstructions of the residual crystallites in potato starch were done using negatives taken from a tilt series in the TEM treated by a low-pass Fourier filter. The helical structure observed three dimensions in stereo mounts and revealed that the organization of lamellae was much more complex than was previously thought to be the case. As a result, they proposed the concept of a 'super helical' structure, which clearly represents a level of structure between that of stacks of lamellae and the granule 'growth' ring.

Debranching studies of starch lends further support to the idea that a blocklet level of structure exists. Hizukuri[15] demonstrated that B-chains of amylopectin can participate in more than one crystalline amylopectin side chain cluster, and proposed a revised model of amylopectin structure, classifying the B-chains according to the number of side chain clusters in which they participate. From this work, it is evident

that B-chains may link the amylopectin side chain clusters to form larger crystalline units. Such evidence corresponds well with the blocklet concept of starch structure. Furthermore, Hizukuri[15] demonstrated that the connecting B-chains were more abundant in potato starch, and proposed that they are probably characteristic of starches with the B-crystal pattern, since such starches have higher amounts of B2–B4 chain fractions. This observation fits with the observation of Gallant et al.[11] that, in general, blocklet size is larger in starches with the B-crystal pattern.

The evidence to date in favor of the blocklet concept of starch granule structure, therefore, indicates that the amylopectin lamellae are organized into effectively spherical blocklets which range in diameter from 20 to 500 nm, depending on starch botanical type and their location in the granule.[1,11,50,136] This organization fits with the current knowledge of starch granule structure and is represented schematically in Figure 5.22. In general, the blocklets are larger (400–500 nm in diameter) in starches of the B- (e.g. potato starch) and C-crystalline types than in starches with the A-crystalline type (e.g. wheat starch, in which the 'blocklets' were 25 to 100 nm in diameter). The large blocklets in potato starch appear to predominate near the granule surface. Consequently, it has been hypothesized that, while granule resistance appears to be linked to several interacting factors, the size of the blocklets (i.e. the degree of local crystallinity) may play a role in starch granule resistance to acid- and enzyme-catalyzed hydrolysis.[11] Blocklet size may, therefore, play a role in the relative resistance of the outer shell of potato starch, and also in the relative resistances of crystalline and semicrystalline growth shells.

Results from every AFM study support the blocklet model. However the blocklet model was newly refined[110] after it was found that contrast, in AFM, was mainly due to localized absorption of water, leading to selective swelling of the matrix material within the starch granule.[124,137] This discovery was the result of a series of studies[107,109,110,124,131] with a goal of comparing near-isogenic pea starches differing in amylose:amylopectin ratio. Structural differences were characterized with AFM, allowing a totally new interpretation of the internal structure of the starch granule. General morphology of the blocklets was imaged using shaded topography and error signal mode images, the matrix being characterized by the force modulation image. The new information leads to the conclusion that the starch granule is composed of continuous hard blocklets dispersed in a softer matrix material. Growth rings are often visible in pea starch granules (wild type, *lam*, and *rug3* low-amylose mutants), but sometimes are missing (high-amylose *r* mutant). Growth rings possibly originate from localized defects in the blocklet production around the surface of spheroidal shells during biosynthesis. In some cases, such as in the *lam* and *rug3* mutants, blocklets are not easily distinguished, and the spheroidal features in the matrix are smaller than the blocklets in parental starch granules. The blocklets may be embedded in a harder interconnecting matrix, possibly amylose in partial crystalline form (high-amylose *r* mutant), or may be enclosed in a hard fine network which encloses a group of blocklets (*rrb* high-amylose mutant).

Thus, each type of starch has its own structural features that now are well-characterized by AFM, using the new, high-resolution technique, which reveals structures much more accurately than in the past. The difficulty remains to determine the

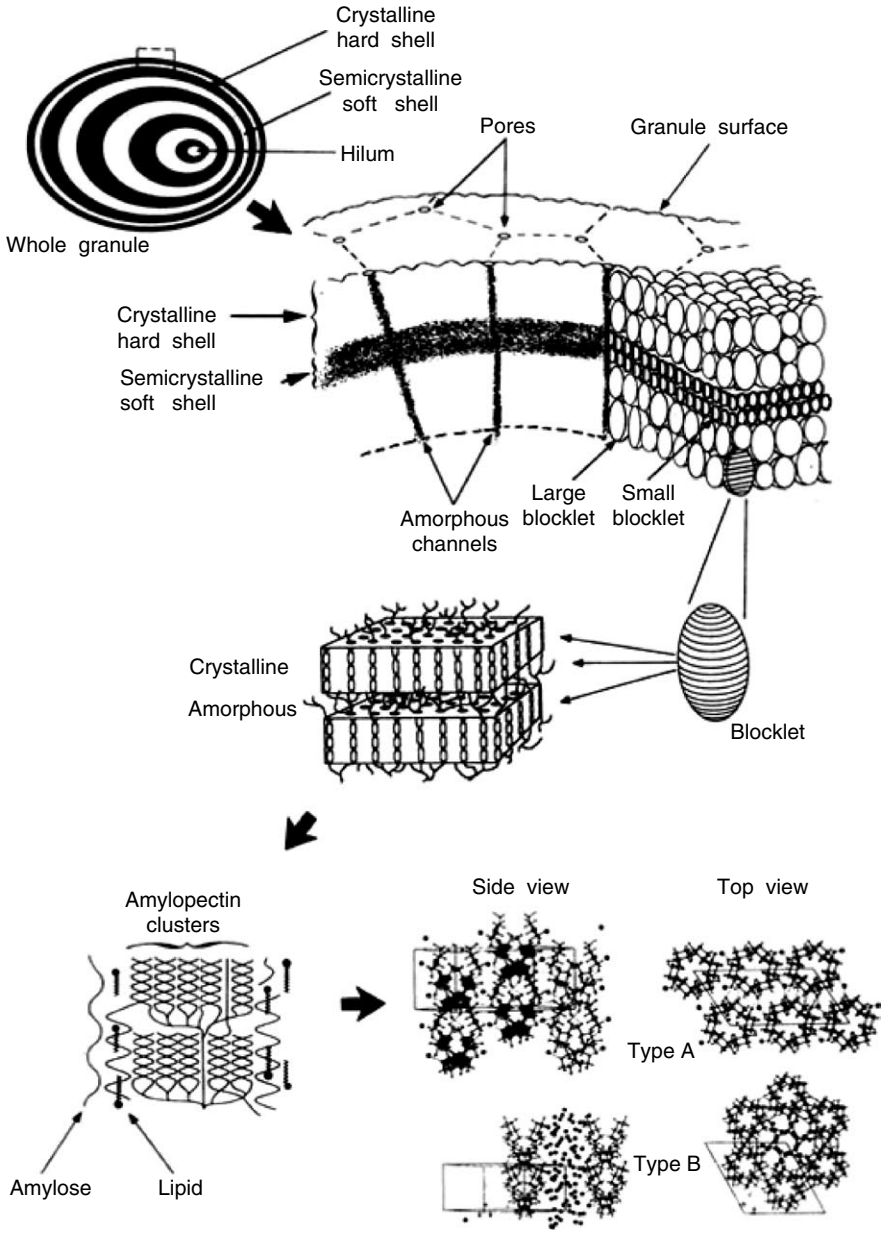

Figure 5.22 Overview of starch granule structure. At the lowest level of granule organization (upper left), alternating crystalline (hard) and semicrystalline (soft) shells are shown (dark and light colors, respectively). Shells are thinner towards the granule exterior (due to increasing surface area to be added to by constant growth rate) and the hilum is shown off-center. At a higher level of structure, the blocklet structure is shown in association with amorphous radial channels. Blocklet size is smaller in the semicrystalline shells than in the crystalline shells. At the next highest level of structure, one blocklet is shown containing several amorphous crystalline lamellae. In the next diagram, amylopectin is shown in the lamellae. The next image is a reminder of the importance of amylose–lipid (and protein) components in the organization of amylopectin chains. At the highest level of order, crystal structures of the starch polymers are shown. (Adapted with permission from reference 1; redrawn in reference 1 from references 32 and 34)

relationship between biochemical data (which gives mean values for the bulk) and data which comes from restricted areas selected under the microscope. Biochemical analysis of smooth pea starch (35% amylose) showed that these starch granules were quite resistant to hydrolysis catalyzed by α-amylase, but a substantial part (amorphous or weakly crystalline) that was more easily solubilized was restricted to the inner parts between the growth rings.[138] Analysis of the β-limit dextrins indicated a significant amount of intermediate branched material (intermediate between amylose and amylopectin) with units of clusters regularly interconnected.[139] The smooth pea granule, a C-type, is a mixture of A-type and B-type crystalline orders. Recording of juxtaposed micro-x-ray diffraction patterns has been performed (thanks to the accuracy of the synchrotron x-ray beam) which demonstrated that the two crystalline phases co-exist within the same granule (Figure 5.9). In the same manner, we may imagine that the accuracy of AFM will soon permit imaging very close areas within such starch granules, thus enabling different types of crystallites to be visualized. Such correspondence between AFM and biochemical data is easier with wrinkled pea starch (64–76% amylose, B-type). Internal areas of the granules are in an amorphous state and parts of the amylose molecules are anchored in the crystalline area.[140] A greater amount of long chain lengths, lower cluster sizes and the presence of intermediate material[141] are elements which could be linked to understand AFM imaging of wrinkled pea starch.

The exact location and organization of amylose in relation to the blocklet organization is not yet known; however, substantial information regarding the location and state of amylose within the granule is beginning to be gathered and is summarized in Section 5.6. The presence of locally more amorphous regions between the blocklets has, however, been visualized by TEM.[11] These regions appear to form amorphous channels between the blocklets. It can be hypothesized that a locally higher concentration of amylose (particularly short chains) may be present in such regions, but consideration of the ratio of amylopectin to amylose (e.g. 75% to 25%) in starch granules and the overall crystallinity (15% to 45%) of starch granules leads to the conclusion that amorphous amylopectin is certainly also present in the amorphous regions of the starch granule.

It is evident from the above discussion that considerable evidence exists for a blocklet level of granule organization between that of the lamellae and the growth rings. Clearly, this level of granule structure has significant implications for the internal architecture (and consequently properties) of starch granules.

VI. Location and State of Amylose Within Granules

Until recently, the location and state of amylose within granules was one of the most important questions remaining to be answered. Three main hypotheses for the location of amylose within starch granules have been put forward. The first hypothesis is that amylose is laid down tangentially to the radial orientation of amylopectin in order to minimize the amylose–amylopectin helical interactions.[142] There is,

however, no experimental basis for such a model, which merely considers the need for amylose and amylopectin to have minimal helical interactions. The other two hypotheses advocate radial deposition of the amylose, either in bundles[43,143] or as individual chains, which are randomly interspersed amongst amylopectin clusters in both crystalline and semicrystalline regions.[144,145] Of the three hypotheses, the third hypothesis appears to be the most sustainable, since it has been demonstrated, via a crosslinking experiment using corn starch, that amylose molecules do not crosslink to one another, but do crosslink to amylopectin chains.[144,145] In order for this crosslinking of amylose with amylopectin to have occurred, hydroxyl groups from the two chains must have been within 7.5 Å of each other.[145] No crosslinking of amylose chains with other amylose chains was observed, which rules out the second hypothesis that amylose chains occur in bundles. The currently accepted model of amylose location in starch granules is, therefore, as individual, radially-orientated chains randomly distributed among the radial amylopectin chains.

There is now substantial evidence indicating that there is an enrichment of amylose towards the periphery of the granule,[64,146–149] and that the amylose molecules found near the surface of the granule have shorter chain lengths than those located nearer the center of the granule.[143] Ring et al.[150] demonstrated that the majority of the amylose in granules can be leached out of granules at temperatures just below the gelatinization temperature. They further demonstrated that the majority of the leached amylose chains were in the single helical state, rather than in a double helical state. The single helical state is, thus, thought to be the predominant state of amylose chains within native starch granules. It is clear, however, from the evidence that amylose can only be completely extracted from granules at temperatures above 90°C,[53] that some large amylose molecules are present within the starch granule, and it is further hypothesized that these larger amylose chains that are not easily leached may participate in double helices with amylopectin.[145]

In association with the enrichment of amylose towards the granule surface, an enrichment of lipid towards (and at) the granule surface is also believed to exist. Evidence in support of this arises from x-ray microanalysis (EDX) and x-ray photoelectron spectroscopy (XPS) which have demonstrated an enrichment of phosphorus (and hence phospholipids at least) towards and at the granule surface.[64,65,151,152] Furthermore, it is now well-established that there is a good correlation between amylose and lipid contents of all normal (i.e. non-mutant) cereal starches.[61,153] Waxy cereal starches (as well as legume and tuber starches) have small amounts of surface lipids and little or no internal lipids, while high-amylose cereal starches tend to have more lipid (most of which is internal) than do the corresponding normal starches.[154] Thus, the quantity of lipid in starch granules appears to be linked to the amylose content, and the lipid appears to be distributed similarly to the amylose. Furthermore, evidence exists that lipid, like the amylose (and amylopectin) polymers, is aligned radially within the granule.[155,156] Both the distribution of the lipid molecules in the granule (which is similar to that of amylose) and its probable radial orientation fit well with evidence that a small proportion of the amylose chains are involved in amylose–lipid complexes. Until recently, evidence for the existence of amylose–lipid complexes in native starch was entirely indirect, arising principally from observations

of the conditions required to extract lipids from starches,[146,157] and from the V-type x-ray diffraction pattern which can be observed with native starches under the right conditions. Direct evidence for the presence of amylose–lipid complexes in native starches has recently been provided by use of (^{13}C-cross-polarization/magic-angle spinning nuclear magnetic resonance (^{13}C-CP/MAS-NMR).[158] Using this technique, it has been demonstrated that amylose–lipid complexes occur in many native cereal starches, including wheat, barley, maize, oat and rice. Comparison of the amylose content of most normal cereal starches (i.e. 25–30%) with the total lipid content of waxy starches (maximum ~1%) suggests that only a small proportion of the amylose in such starches is complexed with lipid. Similarly, it is hypothesized that not all lipid in starch is involved in amylose–lipid complexes and that a free-lipid fraction exists.[156]

In summary, therefore, substantial information regarding the location and state of amylose has been obtained. Individual amylose chains are believed to be randomly located in a radial fashion among the amylopectin molecules. The concentration of amylose (and lipid) increases towards the surface of the granule, with smaller (leachable) amylose chains predominating near the surface. Amylose chains are believed to be in a single helical state, although a small proportion may be involved in lipid complexes.[147] Some of the larger (non-leachable) amylose chains may be involved in double helical interactions with amylopectin.[159]

VII. Surface Pores and Interior Channels of Starch Granules

Small pores, also called 'pin holes', have been observed under SEM on the surface of starch granules. Fannon et al.[84] showed that pores could be found on the granules of corn, sorghum and millet starches, as well as along the equatorial groove of the large granules of wheat, rye and barley starches. Pores were not found on compound starches (rice and oat), nor on tuber and root starches (tapioca, arrowroot, canna and potato). Using SEM and ESEM, they proved in a logical fashion that pores were not artifacts but real features (about 1 μm in diameter) that might be elaborated during granule growth and might be under genetic control.

On the other hand, the surface of the starch granules has been studied by AFM[113–115,130] at high resolution in the non-contact mode, focusing on 'protrusions,' 'depressions' and 'pores.' Depressions 1 μm diameter or less in potato and tapioca starches and pores <100 nm in rice and <40 nm in oat starch granules and in granules of all the cereal starches examined were seen. However, it is impossible to know exactly the depth of the depressions because the 'z' measurements were done from the gray values in the images, unfortunately without any true reference point. But one can wonder if the resolution of this new tool (AFM) is opening a new world of discoveries. Important differences may be observed between high-resolution surface images of starch granules, either performed in the contact mode or in the non-contact mode. In the contact mode, blocklets appear to be of regular shape; in the non-contact mode, the surfaces appear to be very irregular in shape, with plenty of free space or voids.

Fannon et al.[160] suggested that surface pores are openings to channels (5 to 400 nm in diameter) connecting an internal cavity at the granule hilum to the external surface. Studies by Huber and BeMiller[161,162] proved this concept unequivocally. Using waxy maize and sorghum starches and different techniques, e.g. detection of fluorescent dyes and colloidal gold particles by fluorescence microscopy, confocal scanning laser microscopy and by SEM backscattered electron imaging, they proved that these channels and cavities were not filled with amorphous material, but were voids. As mentioned above, only certain starch granules show such openings, suggesting that channels are a predetermined system. One can wonder 'What is the benefit of pores and channels to the plant?' It has been reported that developing and expanding pores were openings to internal corrosion channels with saw-tooth patterns,[90] and that 'these pores may be the site of initial enzyme attack, openings that allow enzyme molecules direct access to the granule interior (hilum) or both.'[84] During the later stages of wrinkled pea starch synthesis, exceptional increase in long chain length occurs. During this stage, the starch granules acquire central fissures. Bertoft et al.[140] suggested that 'soluble starch synthase becomes entrapped at the cracks where it then maintains the synthesis of amylose.' It is possible that pores and channels are related to the control of starch conversion during seed germination[84] or other metabolic activities.

VIII. Conclusions

The intent of this chapter was to start with the polymer composition of starch and continue through the various levels of increasing structural complexity, in order to yield some understanding of the levels of starch granular structure. It has been shown that, with the aid of ever-improving analytical techniques, significant progress has been made in understanding the higher degrees of granule order. The entire picture of starch granule architecture appears to be becoming better understood; however, it should be emphasized that much of the progress made consists of small pieces of information regarding specific features of certain granule structures, and many important questions remain unanswered. For example, it should be remembered that while detailed atomic level models of starch crystal structure have been developed, these only represent a small portion of the granule structure (i.e. the ordered crystalline lamellae containing the double helical amylopectin side chains), since much of the amylopectin in starch is in an amorphous state. From the work of Gidley and Bociek,[48] it is evident that some of this 'amorphous' amylopectin may be in a double helical state; however, the structure of such 'amorphous double helical' amylopectin remains to be described. Similarly, while substantial information regarding the state and location of amylose chains within the granule is now known, numerous further questions regarding the state and location of starch polymers remain. Among these are:

1. Do double helical interactions between amylose and amylopectin chains occur within the granule?
2. Do the semi-amorphous 'growth' shells have a local increase in amylose content (while respecting the general increase in amylose towards the granule surface)?

3. Does amylose disrupt the ordered packing of the amylopectin clusters (i.e. does it play a role in blocklet size)?
4. Are the amylopectin side chains capable of complexing lipids as it was shown in maize starches examined by DSC.[163]

In the course of this chapter, a number of studies of starch have been reviewed. These studies, by revealing substantial new information regarding both the surface chemistry and the structure of the starch granule, highlight the usefulness of applying novel techniques (such as AFM and TOF-SIMS) to examinations of starch. Consequently, it is clear that both surface-specific analysis and scanning-probe microscopy of starch are techniques that can be applied to add to our knowledge of granule structures. Other novel domains may also be considered. In particular, one can envisage using the microdiffraction facilities that synchrotron radiation provides to map the occurrence and the relative orientations of crystalline domains within the same granule. Parallel to these developments, use of chromatographic techniques, in conjunction with enzyme-catalyzed digestion, has provided a detailed description of some essential repeating motifs occurring in starch granules of a given botanical origin. These are the distributions of the lengths of the primary and secondary branches, as well as their attachments onto a main amylosic branch. Unfortunately, existing molecular modeling techniques are not capable of simulating the three-dimensional features of these structures, since they encompass several tens of thousands of atoms. Computing technology is rapidly developing, however, and one can hope that ever-more complex simulations will become possible, thus aiding in the elucidation of the three-dimensional structures of the starch polymers. Via incorporation of biological considerations derived from the structural and functional biology of the different steps of starch biosynthesis (Chapter 4), those computational methods will greatly help in establishing a consistent description and understanding of the several levels of starch structural organization.

As early as 1858, Carl Nägeli stated; 'The starch grain … opens the door to the establishment of a new discipline … the molecular mechanics of organized bodies.'[125] Thus, despite the progress made in understanding starch granule structure, one can appreciate 'Pandora's box' has been opened only slightly, and we are only beginning to explore its boundaries.

IX. References

1. Gallant DJ, Bouchet B, Buléon A, Pérez S. *Eur. J. Clini. Nutr.* 1992;46:S3.
2. Zobel HF. *Starch/Stärke*. 1988;40:44.
3. Oostergetel GT, van Bruggen EFJ. *Carbohydr Polym*. 1993;21:7.
4. Buléon A, Colonna P, Planchot V, Ball S. *Int J Biol Macromol*. 1998;23:85.
5. Nikuni Z. *Chori Kagaku*. 1969;2.
6. French D. *J. Jpn. Soc. Starch Sci.* 1972;19:8.
7. Nikuni Z. *Starch/Stärke*. 1978;30:105.
8. Robin JP, Mercier C, Charbonnière R, Guilbot A. *Cereal. Chem.* 1974;51:389.
9. Manners DJ, Matherson NK. *Carbohydr. Res.* 1981;90:99.
10. Lineback DR. *J. Jpn. Soc. Starch Sci.* 1986;30:80.
11. Gallant DJ, Bouchet B, Baldwin PM. *Carbohydr. Polym.* 1997;32:177.

12. French D. In: Whistler RL, BeMiller JN, Paschall EF, eds. *Starch, Chemistry and Technology*. 2nd edn. Orlando, FL: Academic Press; 1984:184–247.
13. Hizukuri S, Takeda Y, Maruta N, Juliano BO. *Carbohydr. Res.* 1989;189:227.
14. Bertoft E. *Carbohydr. Res.* 1991;212:229.
15. Hizukuri S. *Carbohydr. Res.* 1986;147:342.
16. Manners DJ. *Carbohydr. Polym.* 1989;11:87.
17. Callaghan PT, Lelievre J. *Biopolym.* 1985;24:441.
18. Lelievre J, Lewis JA, Marsden K. *Carbohydr. Res.* 1986;153:195.
19. Callaghan PT, Lelievre J, Lewis JA. *Carbohydr. Res.* 1987;162:33.
20. Yamaguchi M, Kainuma K, French D. *J. Ultrastruc. Res.* 1979;69:249.
21. Gidley MJ, Cooke D. *Biol. Soc. Trans.* 1991;19:551.
22. Sterling CJ. *Polym. Sci.* 1962;56:10.
23. Blanshard JMV, Bates DR, Muhr AH, Worcester DL, Higgins JS. *Carbohydr. Polym.* 1984;4:427.
24. Oostergetel GT, van Bruggen EFJ. *Starch/Stärke*. 1989;41:331.
25. Kassenbeck P. *Starch/Stärke*. 1978;30:40.
26. McDonald AML, Stark JR, Morrison WR, Ellis RP. *J. Cereal Sci.* 1991;13:93.
27. Ring SG, Miles MJ, Morris VJ, Turner R, Colonna P. *Int. J. Biol. Macromol.* 1987; 9:158.
28. Buléon A, Duprat F, Booy FP, Chanzy H. *Carbohydr. Polym.* 1984;4:161.
29. Kregger DR. *Biochem. Biophys. Acta.* 1951;6:406.
30. Wu HCH, Sarko A. *Carbohydr. Res.* 1978;61:27.
31. Wu HCH, Sarko A. *Carbohydr. Res.* 1978;61:7.
32. Imberty A, Chanzy H, Pérez S, Buléon A, Tran V. *J. Mol. Biol.* 1988;201:365.
33. Popov D, Burghammer M, Buléon A, Montesanti N, Putaux JL, Riekel C. *Macromol.* 2006;39:3704.
34. Imberty A, Pérez S. *Biopolym.* 1988;27:1205.
35. Lechert HT. In: Rockland LB, Stewards GF, eds. *Water Activity: Influences on Food Quality*. London, UK: Academic Press; 1981:223–245.
36. Pérez S, Imberty A, Scaringe RP. In: French AD, Brady JW, eds. *Computer Modeling of Carbohydrate Molecules*. Washington, DC: American Chemical Society; 1990:281–289.
37. Pfannemüller B. *Int. J. Biol. Macromol.* 1987;9:105.
38. Gidley MJ, Bulpin PV. *Carbohydr. Res.* 1987;161:291.
39. Gidley MJ. *Carbohydr. Res.* 1987;161:301.
40. Sair L. *Heat-moisture Treatment of Starches*. New York, NY: Academic Press; 1981.
41. Buléon A, Pontoire B, Riekel C, Chanzy H, Helbert W, Vuong R. *Macromol.* 1997;30:3952.
42. Waigh TA, Hopkinson I, Donald AM, Butler MF, Heidelbach F, Riekel C. *Macromol.* 1997;30:3813.
43. Buléon A, Gérard C, Riekel C, Vuong R, Chanzy H. *Macromol.* 1998;31:6605.
44. Bogracheva TY, Morris VJ, Ring SG, Hedley CL. *Biopolym.* 1998;45:323.
45. Imberty A, Pérez S. *Int. J. Biol. Macromol.* 1989;11:177.
46. Jane JL, Wong KS, McPherson AE. *Carbohydr. Res.* 1997;300:219.
47. Gérard C, Planchot V, Colonna P, Bertoft E. *Carbohydr. Res.* 2000;326:130.
48. Gidley MJ, Bociek SM. *J. Am. Chem. Soc.* 1985;107:7040.
49. O'Sullivan AC, Pérez S. *Biopolym.* 1999;50:381.

50. Gallant DJ. [*Doctorat d'Etat*]. Université de Paris VI; 1974.
51. Casset F, Imberty A, Haser R, Payan F, Pérez S. *Eur. J. Biochem.* 1995;232:284.
52. Duprat F, Gallant DJ, Guilbot A, Mercier C, Robin JP. In: Monties B, ed. *Les polymères Végétaux – Polymères pariétaux et alimentaires non azotés*. Paris, France: Gauthier Villars; 1980:176–231.
53. Banks W, Greenwod CT. *Starch and Its Components*. Edinburgh, UK: Edinburgh University Press; 1975.
54. Cauvain SP, Gough BM, Whitehouse ME. *Starch/Stärke*. 1977;29:91.
55. Bowler P, Towersey PJ, Waight SG, Galliard T. In: Hill RD, Münck L, eds. *New Approaches to Research on Cereal Carbohydrates*. Amsterdam, The Netherlands: Elsevier Science; 1985:71–79 .
56. Greenwell P, Evers AD, Gough BM, Russell PL. *J. Cereal. Sci.* 1985;3:279.
57. Nierle W, Bayâ AWE, Kersting HJ, Meyer D. *Starch/Stärke*. 1990;42:471.
58. Baldwin PM. [Ph.D. thesis]. University of Nottingham, UK; 1995.
59. Baldwin PM, Davies MC, Melia CD. *Int. J. Biol. Macromol.* 1997;21:103.
60. Schofield JD, Greenwell P. In: Morton ID, ed. *Cereals in a European Context*. Chichester, UK: Ellis Horwood; 1987:407–420.
61. Morrison WR. *J. Cereal Sci.* 1988;8:1.
62. Goldner WR, Boyer CD. *Starch/Stärke*. 1989;41:250.
63. Swinkels JJM. *Starch/Stärke*. 1985;37:1.
64. Morrison WR, Gadan HJ. *J. Cereal Sci.* 1987;5:263.
65. Malouf RB, Lin WDA, Hoseney RC. *Cereal Chem.* 1992;69:169.
66. Russell PL, Gough BM, Greenwell P, Fowler A, Munro HS. *J. Cereal Sci.* 1987;5:83.
67. Baldwin PM, Melia CD, Davies MC. *J. Cereal Sci.* 1997;26:329.
68. Newman A. *Anal. Chem.* 1996;68:267A.
69. Binnig G, Quaate CF, Gerber C. *Phys. Rev. Lett.* 1986;56:930.
70. Kirby AR, Gunning AP, Morris VJ. *Trends Food Sci. Technol.* 1995;6:359.
71. Hoh JH, Lal R, John SA, Revel J-P, Arnsdorf MF. *Science*. 1991;253:1405.
72. Yang J, Tamm LK, Somlyo AP, Shao Z. *J. Microscopy*. 1993;171:183.
73. Putman CAJ, van der Werf KO, Grooth BGd, van Hulst NF, Greve J. *Biophys. J.* 1994;67:1749.
74. Gunning AP, Kirby AR, Morris VJ, Wells B, Brooker BE. *Polymer Bull.* 1995;615.
75. Yang J, Shao Z. *Micron*. 1995;26:35.
76. Kirby AR, Gunning AP, Morris VJ. *Biopolym.* 1996;38:355.
77. Thomson NH, Miles MJ, Ring SG, Shewry PR, Tatham AS. *J. Vac. Sci. Technol. B, Microelectron. Nanometer Struc.* 1994;12:1565.
78. Hall DM, Sayre JG. *Textile Res. J.* 1969;39:1044.
79. Evers AD. *Starch/Stärke*. 1969;21:96.
80. Hall DM, Sayre JG. *Textile Res. J.* 1970;40:256.
81. Evers AD. *Starch/Stärke*. 1971;23:157.
82. Gallant DJ, Mercier C, Guilbot A. *Cereal Chem.* 1972;49:354.
83. Bowler P, Williams MR, Angold RE. *Starch/Stärke*. 1980;32:186.
84. Fannon JE, Hauber RJ, BeMiller JN. *Cereal Chem.* 1992;69:284.
85. Baldwin PM, Adler J, Davies MC, Melia CD. *Starch/Stärke*. 1994;46:341.
86. Li MJ, Rogers K, Rust CA. *Adv. Mater. Process*. 1995;148:24.
87. Létang C, Piau M, Verdie C. *J. Food Eng.* 1999;41:121.

88. McDonough CM, Rooney LW. *Cereal Food World*. 1999;44:342.
89. Verrez-Bagnis V, Bouchet B, Gallant DJ. *Food Structure*. 1993;12:309.
90. Gallant DJ, Derrien A, Aumaitre A, Guilbot A. *Starch/Stärke*. 1973;25:56.
91. Gallant DJ, Guilbot A. *Starch/Stärke*. 1973;25:335.
92. Fuwa H, Glover D, Sugimoto Y, Tanaka M. *Nutr. Sci. Vitaminol.* 1978;24:437.
93. Fuwa H, Sugimoto Y, Tanaka M, Nikuni Z. *Carbohydr. Res.* 1979;70:233.
94. Pawley J. *J. Microscopy*. 1984;136:45.
95. Hefter J. *Scanning Microscopy*. 1987;1:13.
96. Müllerova I, Lenc M. *Ultramicroscopy*. 1992;41:399.
97. Baldwin PM, Adler J, Davies MC, Melia CD. *J. Cereal Sci.* 1997;21:255.
98. Jahanmir J, Haggar BG, Hayes JB. *Scanning Microscopy*. 1992;6:625.
99. Quate CF. *Surface Sci.* 1994;299–300:980.
100. Blackford BL, Jericho MH, Mulher PJ. *Scanning Microscopy*. 1991;5:907.
101. Weihs TP, Nawaz Z, Jarvis SP, Pethica JB. *Appl. Phys. Lett.* 1991;59:3536.
102. Schwartz UD, Haefke H, Reimann P, Güntherodt HJ. *J. Microscopy*. 1994;173:183.
103. Shakesheff KM, Davies MC, Jackson DE, Roberts CJ, Tendler SJB, Brown VA, Watson RC, Barrett DA, Shaw PN. *Surf. Sci. Lett.* 1994;304:L393.
104. West P, Starostina N. *Advan. Mat., Nanoparticle Technol.* Santa Clara, CA: Pacific Nanotechnology; 2000:1–12.
105. Baldwin PM, Frazier RA, Adler J, Glasbey TO, Keane MP, Roberts CJ, Tendler SJB, Davies MC, Melia CD. *J. Microscopy*. 1996;184:75.
106. Ohtani T, Yoshino T, Hagiwara S, Maekawa T. *Starch/Stärke*. 2000;52:150.
107. Ridout MJ, Gunning AO, Wilson RH, Parker ML, Morris VJ. *Carbohydr. Res.* 2000;50:123.
108. Baker AA, Mervyn JM, Helbert W. *Carbohydr. Res.* 2001;330:249.
109. Morris VJ, Ridout MJ, Parker ML. *Prog. Food Biopolym. Res.* 2005;1:28.
110. Ridout MJ, Parker ML, Hedley CL, Bogracheva TY, Morris VJ. *Carbohydr. Polym.* 2006;65:64.
111. West P, Starostina N. *Advan. Mat., Nanoparticles Technol.* Santa Clara, CA: Pacific Nanotechnology; 2006:1–10.
112. Baldwin PM, Adler J, Davies MC, Melia CD. *Starch/Stärke*. 1995;47:247.
113. Juszczak L. *Electronic J. Polish Agric. Univ.* 2003;6:1.
114. Juszczak L, Fortuna T, Krok F. *Starch/Stärke*. 2003;55:1.
115. Szymonska J, Krok F. *Int. J. Biol. Macromol.* 2003;33:1.
116. Krok F, Szymonska J, Tomasik P, Szymonski M. *Appl. Surf. Sci.* 2000;157:382.
117. Martin C, Smith AM. *Plant Cell*. 1995;7:971.
118. Imberty A, Chanzy H, Pérez S, Buléon A, Tran V. *Macromol.* 1987;20:2634.
119. Ermakov AV, Garfunkel EL. *Rev. Sci. Instrum.* 1994;65:2853.
120. You HX, Lowe CR. *Curr. Opin. Biotechnol.* 1996;7:78.
121. Ollet AL, Kirby AR, Clarke SA, Parker R, Smith AC. *Starch/Stärke*. 1993;45:51.
122. Roberts CJ, Davies MC, Jackson DE, Tendler SJB. *Nanobiol.* 1992;2:73.
123. Goodman FO, Garcia N. *Phy. Rev. B*. 1991;43:4728.
124. Ridout MJ, Parker ML, Hedley CL, Bogracheva TY, Morris VJ. *Biomacromol.* 2004;5:1519.
125. Nägeli CW. In: Schülthess F, ed. *Pflanzenphysiologische Untersuchungen.* Zurich, Switzerland; 1858.

126. Badenhuizen NP. *Protoplasma*. 1937;28:293.
127. Sterling CJ. In: Radley JA, ed. *Starch and Its Derivatives*. 4th edn. London, UK: Chapman and Hall; 1968;139–171.
128. Wetzstein HY, Sterling C. *Stärke*. 1977;29:365.
129. Gallant DJ, Guilbot A. *Stärke*. 1971;23:244.
130. Juszczak L, Fortuna T, Krok F. *Starch/Stärke*. 2003;55:8.
131. Ridout MJ, Parker ML, Hedley CL, Bogracheva TY, Morris VJ. *Carbohydr. Res.* 2003;338:2135.
132. Helbert W, Chanzy H. *Starch/Stärke*. 1996;48:185.
133. Gallant DJ, Guilbot A. *Starch/Stärke*. 1969;21:156.
134. Bertoft E. *Carbohydr. Res.* 1986;149:397.
135. Kassenbeck P. *Starch/Stärke*. 1975;27:217.
136. Gallant DJ, Bouchet BB. *J. Food Microstructure*. 1986;5:141.
137. Morris VJ, Ridout MJ, Parker ML. *Prog. Food Biopolym. Res.* 2005;1:28.
138. Bertoft E, Manelius R, Qin Z. *Starch/Stärke*. 1993;45:215.
139. Bertoft E, Qin Z, Manelius R. *Starch/Stärke*. 1993;45:377.
140. Bertoft E, Manelius R, Qin Z. *Starch/Stärke*. 1993;45:258.
141. Bertoft E, Qin Z, Manelius R. *Starch/Stärke*. 1993;45:420.
142. Gidley MJ. In: Phillips GO, Williams PA, Wedlock DJ, eds. *Gums and Stabilizers for the Food Industry 6*. Oxford, UK: Oxford University Press; 1992:87–99.
143. Zobel HF. In: Alexander RJ, Zobel HF, eds. *Developments in Carbohydrate Chemistry*. St. Paul, MN: American Association of Cereal Chemists; 1992:1–36.
144. Jane JL, Shen JJ. *J. Carbohydr. Chem.* 1993;247:279.
145. Kasemsuwan T, Jane JL. *Cereal Chem.* 1994;71:282.
146. Boyer CD, Shannon JC, Garwood DL, Creech RG. *Cereal Chem.* 1976;53:327.
147. Morrison WR. In: Pomeranz Y, ed. *Advances in Cereal Science and Technology*. St Paul, MN: American Association of Cereal Chemists; 1978;224–348.
148. Schoch TJ. *Meth. Carbohydr. Chem.* 1964;4:25.
149. Shannon JC, Garwood DL. In: Whistler RL, BeMiller JN, Paschall EF, eds. *Starch, Chemistry and Technology*. 2nd edn. Orlando, FL: Academic Press; 1984:26–86 .
150. Ring SG, l'Anson KJ, Morris VJ. *Macromol.* 1985;18:182.
151. Morrison WR. *Starch/Stärke*. 1981;33:408.
152. Morrison WR, Milligan TP. In: Inglett GE, ed. *Maize: Recent Progress in Chemistry and Technology*. New York, NY: Academic Press; 1982:1–18.
153. South JB, Morrison WR, Nelson OE. *J. Cereal Sci.* 1991;14:267.
154. Morrison WR, Milligan TP, Azudin MN. *J. Cereal Sci.* 1984;2:257.
155. Hizukuri S, Nikuni Z. *Nature*. 1957;180:436.
156. Blanshard JMV. *Starch: Properties and Potential, Critical Reports on Applied Chemistry*. Vol. 13. London, UK: Academic Press; 1985:16–54.
157. Morrison WR, Coventry AM. *Starch/Stärke*. 1985;37:83.
158. Morrison WR, Tester RF, Snape CE, Law R, Gidley MJ. *Cereal Chem.* 1993;70:385.
159. Imberty A, Buléon A, Tran V, Pérez S. *Starch/Stärke*. 1991;43:375.
160. Fannon JE, Shull JM, BeMiller JN. *Cereal Chem.* 1993;70:537.
161. Huber KC, BeMiller JN. *Cereal Chem.* 1997;74:537.
162. Huber KC, BeMiller JN. *Carbohydr. Polym.* 2000;41:269.
163. Villwock VK, Eliasson A-C, Silverio J, BeMiller JN. *Cereal Chem.* 1999;76:292.